POLITECNICO DI TORINO

Corso di Laurea in Ingegneria Aerospaziale

Tesi di Laurea

Study on the Origin of Asteroid Oumuamua

Relatori
prof. Lorenzo Casalino
Ir. Ron Noomen
Ir. Sander Elvik

Studente
Andrea Tamburrano
matricola: s251522

Aprile 2020

,

Contents

0.1 Abstract

The discovery over the years of space objects that present uncommon characteristics for most objects in the Solar System, led to the study of these particular objects in order to better understand their nature and try to get information about their place and cause of origin. This project is focused on the study of the asteroid Oumuamua; object Oumuamua was discovered at the end of 2017, after is passage to the perihelion and its origin is unknown because it was detected by telescopes only after approaching our planet. Because of this, we are unable to obtain reliable data on the object under examination before its discovery and it is necessary to rely on "reconstruction" techniques to retrace the trajectory backwards to a possible point of origin. The asteroid Oumuamua has many peculiar characteristics such as a high inclination, hyperbolic orbit (with an eccentricity greater than one) and a high hyperbolic excess of velocity; however, the physical characteristics of this object, such as size, composition and density, are not certain.

The approach used to obtain more information about the origin of Oumuamua was to carry out assessments to identify the orbital and physical parameters of the body; after this it was necessary to evaluate the perturbations that may have diverted its orbit and consider them in the process of propagation of the orbit. Once the orbit was obtained, bodies present in the Solar System were selected, which presented characteristics that could make them possible objects of origin of Oumuamua; these objects were propagated backwards in time and a conjunction analysis with the body under examination was carried out to evaluate their minimum distance.

The analyzes carried out show that none of the 580 candidates is a possible origin for Oumuamua

0.2 Abbreviations

- **AU**: Astronomical Unit
- **i.e.**: Id Est
- **JPL**: Jet Propulsion Laboratory
- **MA**: Minimum Approach
- **MD**: Minimum Distance
- **Pan-STARRS**: Panoramic Survey Telescope and Rapid Response System
- **SRP**: Solar Radiation Pressure
- **UTC**: Universal Time Coordinated
- **w.r.t.**: With Respect To

0.3 Symbols

Latin

Symbol	Meaning	Unit
a	Semi Major Axis	m
a_p	Perturbing Acceleration	m/s^2
e	Eccentricity	Adimensional
E	Eccentric Anomaly	Radiant
h	Orbital Angular Momentum	m^2/s
H	Hyperbolic Anomaly	Radiant
i	Inclination	Radiant
m	Mass	kg
M	Mean Anomaly	Radiant
n	Mean Motion	rad/s
p	Albedo	Adimensional
P	Radiation Pressure	N/m^2
q	Perihelion Distance	m
r	Position	m
$\ddot{r_g}$	Gravitational Acceleration	m/s^2
S	Surface	m^2
t	Time	s
v	Velocity	m/s
v_∞	Hyperbolic Excess Velocity	m/s

Greek

Symbol	Meaning	Unit
ϵ	Specific Orbital Energy	m^2/s^2
μ	Gravitational Parameter	m^3/s^2
ν	True Anomaly	Radiant
ρ	Density	kg/m^3
ω	Argument of Periapsis	Radiant
Ω	Longitude of Ascendin Node	Radiant

Chapter 1

Introduction

The purpose of this thesis is to give a better understanding of the space object known as Oumuamua (or 1I/2017 U1), an interstellar asteroid which was detected at the end of 2017 by a telescope from a Hawaiian observatory. The characteristics of this asteroid make it an interesting case study even though most of its physical characteristic are not known. An object with a hyperbolic trajectory is a good case study because with good odds it may have reached us from a point outside the Solar System and therefore originated outside it. On the other hand, an origin somewhere within the Solar System also can not be ruled out.

The research objective of this study is to determine wheter Oumuamua can have originated somewhere within the Solar System. To achieve this, the first aim of this project is to carry out a preliminary research and analysis to determine the physical characteristics of the body. Once these parameters are found, the next step is to evaluate and determinate which kind of perturbations have a primary effect on the object and with this information choose a method to propagate the trajectory of the asteroid from a certain state (position and velocity) in a specific epoch backward in time. These data can be used in combination with the data obtained from the propagation of the candidates' origins and see if there is a possible match between them.

The current chapter one is focused on introducing the problem, the history of Oumuamua and the process that has been used to develop the project; the second chapter presents the physical parameters of the object and the assessments that are made to assess the uncentainty of these parameters; after that, in Chapter three reports on the preliminary analysis made in order to evaluate the type and amount of perturbations occurring on the asteroid; these are fundamental to be able to choose a perturbation technique (and the integration method) needed to carry out the problem, as reported in Chapter four. Once these considerations are made, Chapter five reports on the preliminary analysis made to discard any doubts about the parameters chosen in the previous chapters. In Chapter six the results obtained from the backward propagation of the asteroid's orbit for different cases are reported. Chapter seven is focused on the study of a possible conjunction between Oumuamua and one of the candidates sources. Finally, chapter eight reports on the conclusions obtained.

Chapter 2

Avaiable data on asteroid Oumuamua

Asteroid Oumuamua (or Asteroid 1I/2017 U1) is a potentially interstellar object that was first detected on the 18th of October 2017 by Rob Weryk, a member of the team that works at Pan-STARRS (Panoramic Survey Telescope and Rapid Response System).The name Oumuamua, which comes from the Hawaiian language, means 'scout' (from ou, meaning 'reach out for', and mua, reduplicated for emphasis, meaning 'first'). It can be translated as 'first distant messenger' [**4**].
This object has a hyperbolic trajectory, a very strange characteristic for an object in the Solar System; the asteroid reached its minimum distance from the Sun of 0.25 AU on the 9th of September 2017 and the minimum distance from Earth of 0.16 AU on the 14th of October 2017, four days before being discovered [**4**].
It seems to come from a place in the constellation of Lyra and, after passing the perihelion, it changed its trajectory towards the constellation of Pegasus.
It was difficult to classify it, because of its small dimension and because it was detected on its way out , so it was farther from us every day. Thanks to observations of its light curve, it is possible to say that it has an elongated shape and it rotates around a non-principal axis with a type of movement known as *tumbling*. It has a hyperbolic excess velocity (v_∞) of 26.33 km/s, much higher than any other objects observed in the Solar System with an eccentricity greater than one.
Initially it was thought that it could be a comet, due to its hyperbolic orbit (characteristic of many comets) but, after observations made by the Very Large Telescope, no presence of a Coma was identified (a Coma is a nebulous envelope around the nucleus of a comet, formed when the comet passes close to the Sun in its orbit; as the comet warms, parts of it sublimate. This gives a comet a "fuzzy" appearance when viewed in telescopes and distinguishes it from stars [**8**]). After these evaluations it was re-designated as an asteroid.

2.1 Orbital Parameters

The orbital parameters (or Keplerian orbital elements) are a set of parameters necessary to uniquely determine an orbit, given an ideal system consisting of two masses that follow the Newtonian laws of motion and the law of universal gravitation. It is possible to describe a central motion in different ways depending on the variables that one chooses to identify it, but all these methods uniquely define the same orbit. The ways in which an orbit can be defined are:

- the six orbital parameters;
- the vector constants of motion, i.e. the specific orbital angular momentum $\boldsymbol{h}$, the vector eccentricity $\boldsymbol{e}$ and the specific orbital energy $\boldsymbol{\varepsilon}$;
- the two orbital state vectors: the position vector $\boldsymbol{r}$ and the velocity vector $\boldsymbol{v}$.

The six orbital parameters are:

- Inclination $\boldsymbol{i}$;
- Longitude of the ascending node $\boldsymbol{\Omega}$;
- Argument of periapsis $\boldsymbol{\omega}$;
- True-anomaly $\boldsymbol{\nu}$;
- Semimajor axis $\boldsymbol{a}$;
- Eccentricity $\boldsymbol{e}$.

The orbital parameters are represented in *Figure 2.1*[**9**] :

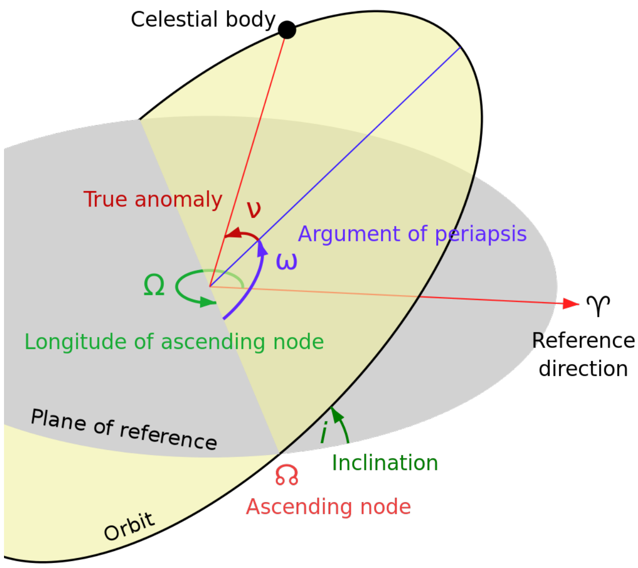

Figure 2.1: Orbital Parameters[**9**]

Thanks to the *JPL Small-Body Database Browser*, it is possible to obtain information of a large number of (known) celestial bodies.
It is also possible to obtain the orbital parameters of the body Oumuamua at a determinate moment of time; in this case the observation time is 23 November 2017 00:00 UTC (JD:2458080) **[1]** and the data are shown in Table *2.1*:

Data	Value	Uncertainty	Units	Name
e	1.201	$2.106*10^{-5}$		eccentricity
i	122.742	$2.883*10^{-4}$	deg	inclination
q	0.256	$6.664*10^{-5}$	AU	perihelion distance
a	-1.272	$1.002*10^{-4}$	AU	semi-major axis
Tp	2017-Sep-09 12:10:32	$2.642*10^{-4}$	TDB	time of perihelion passage
	2,458,006.0073 JD			
ω	241.811	1.250	deg	argument of perihelion
Ω	24.597	$2.542*10^{-4}$	deg	longitude of the ascending node
M	51.158	$6.116*10^{-3}$	deg	mean anomaly
n	0.687	$8.108*10^{-5}$	deg/day	mean motion

Table 2.1: Orbital Parameters of Oumuamua**[1]**

This asteroid has a hyperbolic trajectory, very unusual for bodies in the Solar System. Assuming that it is indeed an interstellar object, it entered the Solar System from north of the plane of the ecliptic; thanks to the gravity of the Sun it increased his velocity until it reached its maximum velocity of 87.71 km/s, as it passed south of the ecliptic (on 6 September 2017) and made a sharp turn northward at its closest approach to the Sun (perihelion, on 9 September 2017) at a distance of 0.255 AU from the Sun. The object is now heading away from the Sun towards Pegasus. It will continue to slow down until it reaches a velocity of 26.33 km/s relative to the Sun (at a distance of 427.66 AU), the same velocity it had before its approach to the Solar System, assuming it arrived from out the Solar System. The trajectory is illustrated in Figure *2.2* **[2]**:

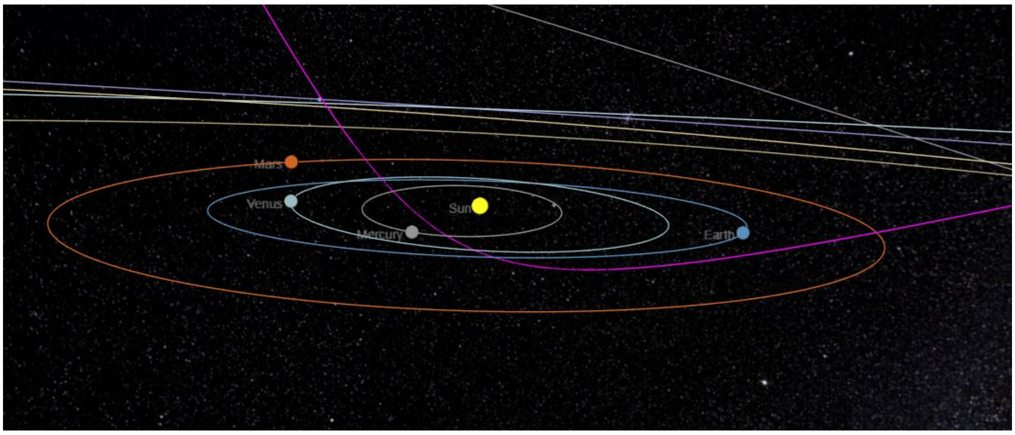

Figure 2.2: Trajectory of Oumuamua (inclinated curve), with that of the planets **[2]**

2.2 Dimensions

In addition to the orbital parameters it is necessary to know other physical characteristics of the object, such as dimensions and composition.
It is very hard to determine the real dimensions of this body, because it is very small compared to the characteristic lengths of the space environment and it has a very high velocity; these characteristics make it difficult to be studied by telescopes and spectrometers. Thanks to the analysis made on the variations of light reflected on this body, we can say that Oumuamua can be either a highly elongated object or an extremely flat object. In order to determinate the dimensions, scientists related the amount of albedo and two hypothetical physical models (cigar-shape, 1:8 aspect ratio; disc-shape, 1:6 ratio) and did assumptions on that. We can use two models for the object, with the dimension shown in Table *2.2* [**5**] :

Model	a [m]	b [m]	c [m]	p
Disc	111	115	19	0.1
Cigar	320	50	40	0.1

Table 2.2: Dimensions for the two shapes [**5**]

The parameter p is the albedo, a measure of the diffuse reflection of solar radiation out of the total solar radiation received by an astronomical body. It is dimensionless and measured on a scale from 0, corresponding to a black body that absorbs all incident radiation, to 1, corresponding to a body that reflects all incident radiation.
Below one can see the two configurations in Figure *2.4* and Figure *2.3*, respectively:

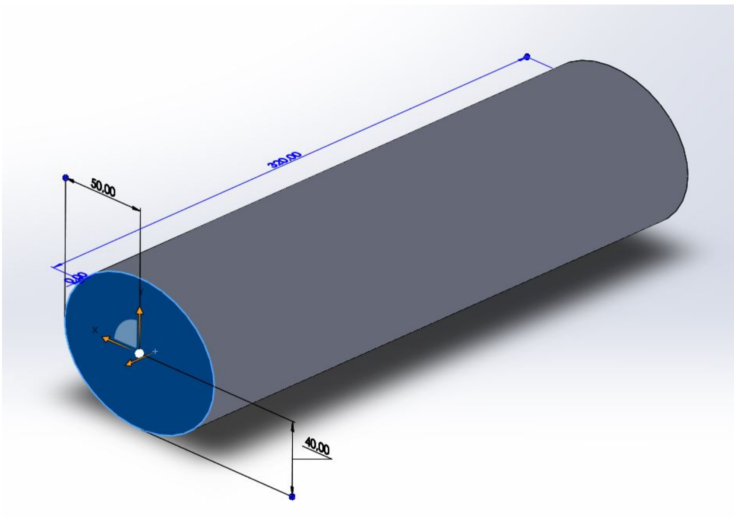

Figure 2.3: Cigar-Shape of the object

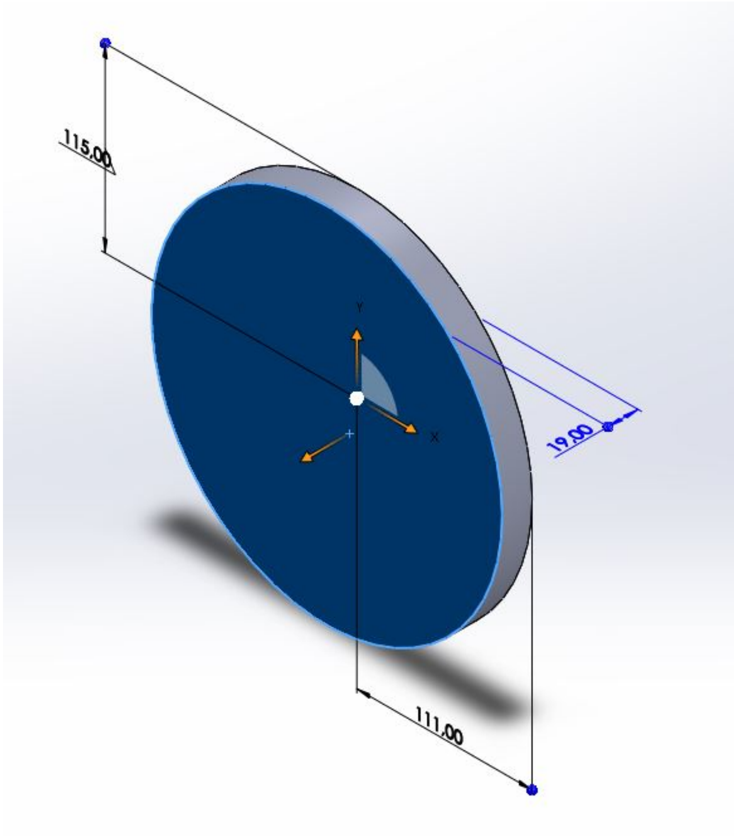

Figure 2.4: Disc-Shape of the object

2.3 Composition

The composition of the object in unknown, spectral analysis shows that the object should be colored red, like a Kuiper belt object. It has a spectrum similar to that of *D-type* asteroid, a class of asteroids with a very low albedo and with a reddish spectrum; it has been suggested that they have a composition of organic-rich silicates, carbon and anhydrous silicates, possibly with water ice in their interiors [**2**].
The object is rotating around a non-principal axis, a type of movement known as *tumbling*, with a rotation period of 8.10 hours (for uncertainties there are two models, respectively ± 0.42 hours or ± 0.02 hours). Since we do not have reliable data confirming its internal composition, it is not possible to determine its density with certainty; for this reason more cases with different densities will have to be analyzed.Options are:

- composed by dust, with a density $\rho = 10^3$ kg/m^3;
- composed by icy dust, with $\rho = 10^{-5}$ kg/m^3;
- the same density as usual comets, with $\rho = 0.6 * 10^3$ kg/m^3;
- the same density as usual asteroids, with $\rho = 2 * 10^3$ kg/m^3;

Chapter 3

Orbital Mechanics

Once the characteristic parameters (phisical and geometric) of the body under examination have been obtained, it is necessary to determine the perturbative effects that act on it; these are necessary to evaluate how much the real trajectory differs from an unperturbed one, that is, the one that the body would have if it were subject only to the gravitational attraction force of the Sun.
There are many kinds of perturbations:

- Third-body perturbations;
- Solar radiation pressure;
- Atmospheric drag;
- Effect of imperfect sphericity of the main body;
- Propulsion;
- Magnetic fields.

In this case, the atmospheric drag is not considered, as the asteroid keeps such a distance from the planets that have an atmosphere that this effect does not affect the body; the same principle applies to the effect of the non-sphericity of the planets and magnetic fields, as these effects are predominant when the asteroid is in the vicinity of the perturbing body. The effect of propulsion is not considered because an asteroid, unless there are effects due to sublimation of some parts of it, does not have propulsive effects. In order to quantify these remaining perturbations we can calculate the perturbative accelerations.

3.1 Third-Body Perturbations

This kind of perturbations are due to the presence of one or more secondary bodies which exert an attractive force on the object that is in orbit around a main body. Typically, only a spherical point-mass gravity model is used for modeling effects from these so-called third bodies.

The system used is heliocentric ecliptic coordinates. The perturbing aceleration, a_p, has been calculated using Equation (3.1):

$$a_p = \mu \frac{r}{R^3} \sqrt{(1 + 3cos(\beta))} \tag{3.1}$$

r is the distance between the Sun and Oumuamua, R is the distance between the Sun and the perturbing planet, μ is the gravitational parameter of the perturbing planet and β is the angle between $\bar{r}$ and $\bar{R}$. This calculation has been made for different planets, at the moment of closest approach with object Oumuamua. In Figure *3.1* is shonw the reference system:

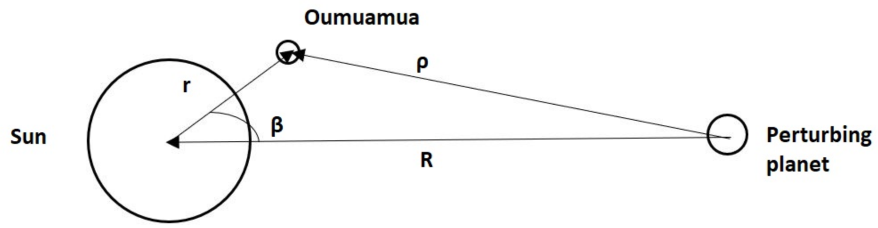

Figure 3.1: Reference system

3.1.1 Earth

In this case the moment was chosen when Oumuamua had its closest approach to the Earth, the 15/10/2017 03:00 UTC. The data are taken from [**1**]:

- Oumuamua-Sun distance (r)=1.14 AU;
- Sun-Earth distance (R)=1 AU;
- Earth-Oumuamua distance (ρ)=0.162 AU.

The angle β was calculated with Equation (3.2) derived from the Carnot theorem:

$$\beta = \arccos \frac{R^2 - \rho^2 + r^2}{2Rr} \tag{3.2}$$

and with Equation (3.1) was found:

$a_p = 4.0035 * 10^{-11}$ km/s^2

3.1.2 Mercury

In this case the moment was chosen when Oumuamua had its closest approach to Mercury, the 15/09/2017 05:00 UTC. In this case were known:

- Oumuamua-Sun distance (r)=0.326 AU;
- Mercury-Sun distance (R)=0.387 AU;

In order to find the distance between Oumuamua and Mercury the ephemeris were used; with the Right Ascension and Declination found on **[1]** it was possible to calculate $\bar{r}$ and $\bar{R}$ and with the relation (3.3) :

$$\bar{\rho} = \bar{R} + \bar{r} \tag{3.3}$$

With Equation (3.2) and (3.1) it was found:

$a_p = 8.0846 * 10^{-12}$ km/s^2

3.1.3 Venus

In this case the moment was chosen when Oumuamua had its closest approach to Venus, the 11/09/2017 07:00 UTC. In this case were known:

- Oumuamua-Sun distance (r)=0.263 AU;
- Venus-Sun distance (R)=0.715 AU;

In order to find the distance between Oumuamua and Venus the ephemeris were used the Ephemeris; with the Right Ascension and Declination found on **[1]** it was possible to calculate $\bar{r}$ and $\bar{R}$ and with the relation (3.3) we can find ρ. With Equation (3.2) and (3.1) it was found:

$a_p = 7.4352 * 10^{-13}$ km/s^2

3.1.4 Jupiter

In this case the moment was chosen when Oumuamua had its closest approach to Jupiter, the 15/08/2017 00:00 UTC. In this case were known:

- Oumuamua-Sun distance (r)=0.856 AU;
- Jupiter-Sun distance (R)=5.448 AU;

In order to find the distance between Oumuamua and Jupiter the ephemeris were used; with the Right Ascension and Declination found on **[1]** it was possible to calculate $\bar{r}$ and $\bar{R}$ and with the relation (3.3) we can find ρ. With Equations (3.2) and (3.1) it was found:

$a_p = 4.393 * 10^{-11}$ km/s^2

3.1.5 Saturn

In this case the moment was chosen when the Asteroid Oumuamua had its closest approach to Saturn, the 07/05/2017 00:00 UTC. In this case were known:

- Oumuamua-Sun distance (r)=3.095 AU;
- Saturn-Sun distance (R)=10.02 AU;

In order to find the distance between Oumuamua and Saturn the ephemeris were used; with the Right Ascension and Declination found on [**1**] it was possible to calculate $\bar{r}$ and $\bar{R}$ and with the relation (3.3) we can find ρ. With Equations (3.2) and (3.1) it was found:

$a_p = 5.7873 * 10^{-12}$ km/s^2

3.2 Solar Radiation Pressure

The surface of the object is hit by a beam of photons and the temperature increases; moreover there is an exchange of momentum between the object and the Sun's emitted photons. Normally, the forces generated by radiation pressure are too small to be noticed under everyday circumstances; however, in space this is one of the main forces acting on objects, besides gravity, and the net effect of a tiny force may produce a large cumulative effect over long periods of time.
The interaction of electromagnetic waves (or photons) with matter involves an exchange of momentum. Due to the law of *Conservation of Momentum*, any change in the total momentum of the waves (or photons) must involve an equal and opposite change in the momentum of the matter it interacted with (*Newton's Third Law of Motion*)[**3**].
Equation (3.4)[**6**] can be used to evaluate the magnitude of the acceleration:

$$a_p = P\frac{S}{m} \tag{3.4}$$

where S is the cross-sectional area of the object perpendicular to the direction to the Sun, m is the mass of the object and P the radiation pressure. In this case, at the closest approach of Oumuamua to the Sun, we have a distance of 0.25 AU and for this value:

$P = 73\ \mu N/m^2$

In this case different assumptions were done:

- the calculations have been made for both the Cigar and Disc shape;
- were considered two different densities ($10^3 kg/m^3$ and $10^{-5} kg/m^3$);
- the calculation has been made in the best case, when the surface perpendicular to the direction to the Sun is smallest and the worst case, in which the surface perpendicular to the direction to the Sun is largest;

The density values used are:

- $\rho_1 = 10^3$ kg/m^3
- $\rho_2 = 10^{-5}$ kg/m^3

3.2.1 Best case

In this case the surfaces perpendicular to the direction to the Sun are:

- $S_d = 6.8644 * 10^3$ m^2
- $S_c = 6.2832 * 10^3$ m^2

With this value it is possible to calculate the values in Table *3.1*:

Model	$a_p(\rho_1)$ [km/s^2]	$a_p(\rho_2)$ [km/s^2]
Disc	1.02*10^{-9}	0.102
Cigar	3.55*10^{-10}	0.0355

Table 3.1: Perturbative solar radiation pressure acceleration-Best case

3.2.2 Worst case

In this case the surfaces perpendicular to the direction to the Sun are:

- $S_d = 4.01024 * 10^4$ m^2
- $S_c = 5.02655 * 10^4$ m^2

With this values it is possible to calculate the values in Table *3.2*:

Model	$a_p(\rho_1)$ [km/s^2]	$a_p(\rho_2)$ [km/s^2]
Disc	5.97*10^{-9}	0.597
Cigar	2.84*10^{-9}	0.284

Table 3.2: Perturbative solar radiation pressure acceleration-Worst case

3.3 Analysis of the Results

Once having evaluated the perturbative accelerations for different cases, it is possible to compare them to the acceleration the object has due to the gravity force of the Sun, in order to understand how these affect the dynamics of the body.

3.3.1 Third-Body Effect

It is possible to use Equation (3.5) in order to evaluate which one of the two accelerations has a major impact on the total acceleration ($\ddot{\bar{r}}$) ;

$$\ddot{\bar{r}} = -\frac{\mu_s}{r^2}\frac{\bar{r}}{|\bar{r}|} + \bar{a}_p \tag{3.5}$$

$\bar{r}$ is the distance vector from the Sun to Oumuamua, μ_s is the standard gravitational parameter of the Sun and $\bar{r}_{Sun} = -\frac{\mu_s}{r^2}\frac{\bar{r}}{|\bar{r}|}$ is the gravitational acceleration due to the Sun.

In Table *3.3* it is possible to see the influence of the perturbative acceleration:

Planet	a_p [km/s^2]	r_g [km/s^2]	$\frac{a_p}{r_g}$
Earth	$4*10^{-11}$	$4.56*10^{-6}$	$8.77*10^{-6}$
Mercury	$8.08*10^{-12}$	$5.58*10^{-5}$	$1.45*10^{-7}$
Venus	$7.44*10^{-13}$	$8.57*10^{-5}$	$8.68*10^{-11}$
Jupiter	$4.40*10^{-11}$	$8.09*10^{-6}$	$5.44*10^{-6}$
Saturn	$5.79*10^{-12}$	$6.2*10^{-7}$	$9.34*10^{-6}$

Table 3.3: Comparison of accelerations.

As we can see from the ratio $\frac{a_p}{r_g}$, the perturbative effect due to the presence of other planets is not influential on the total acceleration of the asteroid.

3.3.2 Solar Radiation Pressure Effect

Using Equation (3.5) it is possible to evaluate which one of the two accelerations has a major impact on the total acceleration ($\ddot{r}$), in both cases; in Table *3.4* there are the data of the best case and in Table *3.5* the ones of the worst case:

Model	$a_p(\rho_1)$ [km/s^2]	$a_p(\rho_2)$ [km/s^2]	r_g [km/s^2]	$\frac{a_p(\rho_1)}{r_g}$	$\frac{a_p(\rho_2)}{r_g}$
Disc	$1.02*10^{-9}$	0.102252	$9.05*10^{-5}$	$1.13*10^{-5}$	1127.1
Cigar	$3.55*10^{-10}$	0.035469	$9.05*10^{-5}$	$3.92*10^{-6}$	391.92

Table 3.4: Perturbative solar radiation pressure acceleration effect in the best case.

Model	$a_p(\rho_1)$ [km/s^2]	$a_p(\rho_2)$[km/s^2]	r_g [km/s^2]	$\frac{a_p(\rho_1)}{r_g}$	$\frac{a_p(\rho_2)}{r_g}$
Disc	$5.97*10^{-9}$	0.597	$9.05*10^{-5}$	6.60^{-5}	6596.70
Cigar	$2.84*10^{-19}$	0.284	$9.05*10^{-5}$	$3.14*10^{-5}$	3138.12

Table 3.5: Perturbative solar radiation pressure acceleration effect in the worst case.

It is possible to see how the two different densities cause different effects on the body; in both cases the objects (both cigar-shape and disc-shape) with high density are not so perturbed from the Solar Radiation Pressure; the ones with low density have a very high $\frac{a_p(\rho_2)}{r_g}$ value and this means that the perturbative effect due to Solar radiation pressure is very intense.

Chapter 4

Propagation Techniques

In this chapter the approach of the study of perturbations will be discussed by the use of perturbation techniques; there are two main categories of perturbation techniques:

- *Special perturbation techniques*: they deal with the direct numerical integration of the equation of motion, including all necessary perturbing accelerations;
- *General (or absolute) perturbation techniques*: they involve an analytic integration of series expansion of the perturbing accelerations. This is a more difficult and lengthy technique than the other one, but it gives a better understanding of the effect of the perturbation.

Some cases of *special perturbation techniques* are now reported.

4.1 Cowell's Method

This is a method which needs to write the equation of motion, including the perturbations, and then integrate them step by step. Having the analytical formulation of the perturbation, the state vector (comprising $\bar{r}$ and $\dot{\bar{r}}$) at any time can be found by applying one of the numerical integration schemes at Equations (4.1) **[6]**:

$$\begin{cases} \dot{x} = v_x \\ \dot{y} = v_y \\ \dot{z} = v_z \\ \dot{v}_x = a_{px} - \frac{\mu}{r^3} x \\ \dot{v}_y = a_{py} - \frac{\mu}{r^3} y \\ \dot{v}_z = a_{pz} - \frac{\mu}{r^3} z \end{cases} \tag{4.1}$$

The method has a simple formulation and implementation and is possible to handle multiple perturbations at the same time.
There are some disadvantages:

- it needs small integration steps when the object is near a large attraction body;
- it is slower than other methods (ten times slower than Enke's method).

4.2 Enke's Method

With this method the sum of all accelerations is integrated together; it integrates the difference between the primary acceleration and the perturbing acceleration. In this case we have a reference orbit without perturbations called *osculating orbit*, and the real orbit. At any epoch, if all the perturbations were to stop acting, the *osculating orbit* is what is found. When the two (with and without perturbations) are too different, there is a process called rectification; this means that a new starting point will be chosen which will coincide with the true orbital path. Than a new *osculating orbit* is calculated. It is integrated:

$$\bar{\delta\ddot{r}} = \bar{a}_p + \frac{\mu}{\bar{\rho}^3}[(1 - \frac{\bar{\rho}^3}{\bar{r}^3})\bar{r} - \bar{\delta r}] \tag{4.2}$$

$$\bar{\delta r} = \bar{r} - \bar{\rho}$$

$\bar{r}$ is the position vector of the real orbit, $\bar{\rho}$ is the position vector of the *osculating orbit*; knowing $\bar{\rho}$ at a determinate epoch, is possible to calculate $\bar{r}$ and $\bar{\ddot{r}}$.

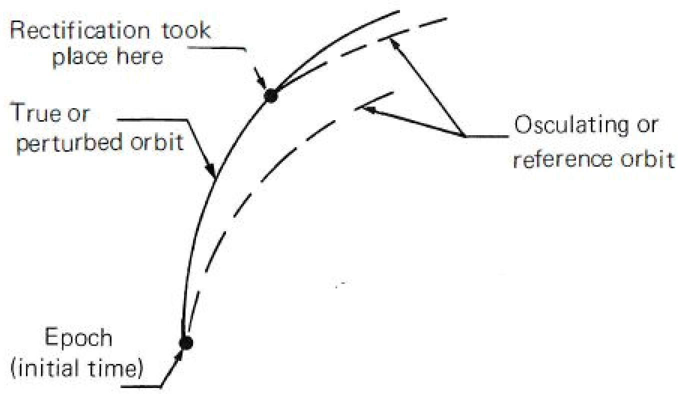

Figure 4.1: Osculating orbit **[6]**

When the value of $\frac{\delta r}{\rho}$ is higher than a default value, e.g. 1%, a new *osculating orbit* has to be calculated starting from that epoch. In this case there will be a change in Kepler elements. The true orbit is a succession of *osculating orbits*

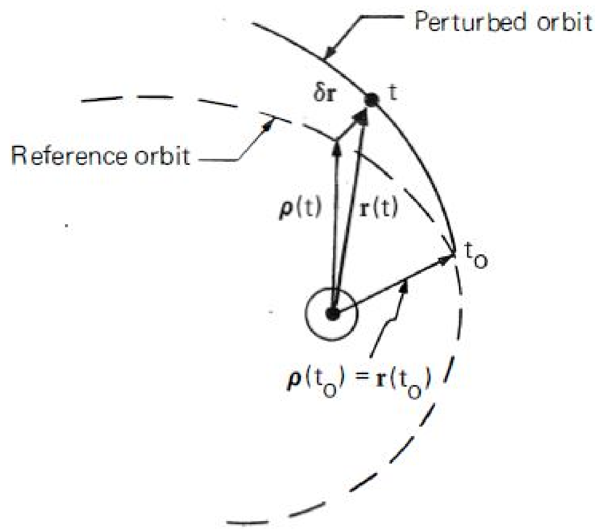

Figure 4.2: Deviation from the reference orbit [**6**]

4.3 Classical Orbital Elements Variation

These methods are good when the perturbing accelerations are small. At any time, if the real $\bar{r}$ and $\dot{\bar{r}}$ are known, it is possible to see how the orbital parameters change, even if the variation is very small, due to the perturbations. Since the rate of change is small, it is possible to take bigger steps of integration.
This approach uses the R-S-W system, where R is the direction from the main planet towards the object; S is in-plane and rotated of 90° from R in the direction of increasing M (mean anomaly); W is perpendicular to both R and S. The reference system is shown in Figure *4.3*:

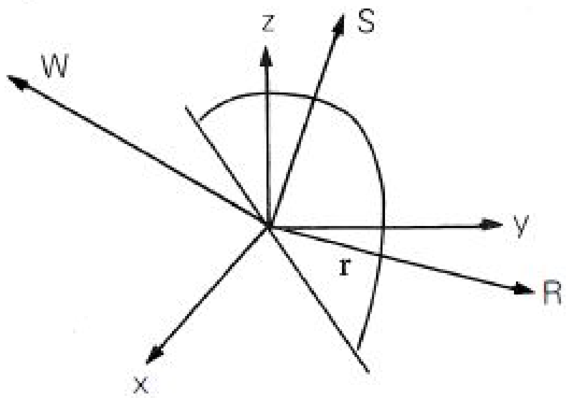

Figure 4.3: R-S-W reference system [**6**]

After writing the equation for the values:

$$\begin{cases} \frac{da}{dt} \\ \frac{de}{dt} \\ \frac{di}{dt} \\ \frac{d\Omega}{dt} \\ \frac{d\omega}{dt} \\ \frac{dM}{dt} \end{cases}$$

These equations are shown in Figure *4.4*:

$$\frac{da}{dt} = \frac{2e \sin \nu}{n\sqrt{1-e^2}} F_r + \frac{2a\sqrt{1-e^2}}{nr} F_s$$

$$\frac{de}{dt} = \frac{\sqrt{1-e^2} \sin \nu}{na} F_r + \frac{\sqrt{1-e^2}}{na^2 e} \left[\frac{a^2(1-e^2)}{r} - r \right] F_s.$$

$$\frac{di}{dt} = \frac{r F_W \cos u}{na^2\sqrt{1-e^2}}$$

$$\frac{d\Omega}{dt} = \frac{r F_W \sin u}{na^2\sqrt{1-e^2} \sin i}$$

$$\frac{d\omega}{dt} = \left(\frac{d\omega}{dt}\right)_r + \left(\frac{d\omega}{dt}\right)_s + \left(\frac{d\omega}{dt}\right)_w$$

$$\left(\frac{d\omega}{dt}\right)_r = -\frac{\sqrt{1-e^2} \cos \nu}{nae} F_r$$

$$\left(\frac{d\omega}{dt}\right)_s = \frac{p}{eh} \left[\sin \nu \left(1 + \frac{1}{1+e\cos \nu}\right)\right] F_s$$

$$\left(\frac{d\omega}{dt}\right)_w = -\frac{r \cot i \sin u}{na^2\sqrt{1-e^2}} F_W$$

$$\frac{dMo}{dt} = -\frac{1}{na} \left(\frac{2r}{a} - \frac{1-e^2}{e} \cos \nu\right) F_r$$

$$-\frac{(1-e^2)}{nae} \left(1 + \frac{r}{a(1-e^2)}\right) \sin \nu F_s - t \frac{dn}{dt},$$

Figure 4.4: Laplace Equations [**6**]

It is necessary to calculate the 6 orbital parameters a $t = t_0$ and the perturbation force in the RSW system. Then the six rates-of-change for the elements have to be calculated and the equations have to be integrated numerically. With the new parameters it is possible to calculate the new $\bar{r}$ and $\dot{\bar{r}}$. This procedure has to be done until the final time is reached.
This procedure has some limits:

- it has problems for e=0 and e=1;
- the value of $\frac{dM}{dt}$ has to be calculated based on the type of conic;

4.4 Integration Method

Numerical integration methods can be divided into single-step and multi-step categories. The multi-step methods usually require a single step-method to start them at the beginning and after each step-size change.

4.4.1 Runge-Kutta Method

It is one of the most common integration methods; it is usually used to start the multi-step methods. It uses an approximation of Taylor series extrapolation **[6]**. The equation for a fourth-order method is :

$$\bar{x}_{n+1} = \bar{x}_n + 1/6(k_1 + 2k_2 + 2k_3 + k_4) \tag{4.3}$$

where:

$$\begin{cases} k_1 = hf(t_n, \bar{x}_n) \\ k_2 = hf(t_n + h/2, \bar{x}_n + k_1/2) \\ k_3 = hf(t_n + h/2, \bar{x}_n + k_2/2) \\ k_4 = hf(t_n + h, \bar{x}_n + k_3) \end{cases}$$

h is the step-size, n is the increment number and $f(t_n, \bar{x}_n)$ is the function that describes the problem.

4.4.2 Adams-Moulton Formulas

This technique implements a corrector formula to the normal equation. It requires a single-step method to start the integration. The predictor formula is:

$${x_{n+1}}^{\mathrm{P}} = x_n + h/24(55f_n - 59f_{n-1} + 37f_{n-2} - 9f_{n-3}) + 251/270h^5 \frac{d^5x(\xi)}{dt^5} \tag{4.4}$$

while the corrector is:

$${x_{n+1}}^{\mathrm{C}} = x_n + h/24(9f_{n+1} + 19f_n - 5f_{n-1} + 9f_{n-2}) + 19/270h^5 \frac{d^5x(\xi)}{dt^5} \tag{4.5}$$

the last term in each equation is the truncation error term. In Equation (4.5) the term $f_{n+1}$is found from the predicted value:

$$f_{n+1} = f(t_{n+1}, {\bar{x}_{n+1}}^{\mathrm{P}}) \tag{4.6}$$

4.5 Evaluation of the methods

For this problem the Cowell's Method will be used, since others methods have to have a shorter steps due to the potential presence of high perturbations, such as for the low density SRP case; the Runge-Kutta Method will be used as integration method because of its easy implementation and good accuracy.

Chapter 5

Preliminary Analysis

In order to evaluate if all the configurations identified so far in this project are possible, the unperturbed trajectory will be propagated from the 23/11/2017 (the epoch to which the orbital parameters available on JPL refer), in order to have a better precision, and will be compared with the data available in [**1**]; the avaiable data were derived from observations carried out for 80 days (from 14/10/2017 to 2/1/2018), with a total of 207 observations.
The values of the state vector of Oumuamua (taken on [**1**]) refer to a period of time from the 1/1/2017 till 23/11/2017, the period in which the asteroid was closest to the inner planets of the Solar System and the ecliptic plane, with a gap of 1 day.

5.1 Unperturbed Trajectory

To propagate the orbit it is necessary to start from a known point of the orbit, in this case the epoch to which the asteroid's orbital parameters refer; knowing the value of the *mean motion (n)* it is possible to obtain the *mean anomaly (M)* by using Equation (5.1); in this case M_i in the mean anomaly referred to 23/11/2017 and t it the time span (in this case 1 day).
Making use of *Newton Iteration for Hyperbolic Anomaly* (5.2), it is possible to start an iteration in order to find at every epoch the *Hyperbolic Anomaly (H)* and with Equation (5.3) the value of the range of the object;

$$M_t = M_i + n * t \tag{5.1}$$

$$H_{k+1} = H_k + \frac{M - esinh(H_k) + H_k}{ecosh(H_k) - 1} \tag{5.2}$$

$$r(t) = a(1 - ecosh(H(t))) \tag{5.3}$$

With the relation (5.4) it is possible to obtain the *True Anomaly (ν)* and with Equation (5.5) it is possible to obtain the coordinates of the object in the *Perifocal Plane.*

$$r(t) = \frac{a(1-e^2)}{1+ecos(\nu(t))} \tag{5.4}$$

$$\begin{cases} x_p = rcos(\nu); \\ y_q = rsin(\nu); \end{cases} \tag{5.5}$$

Thanks to the transformation matrix (5.6) and the relation (5.7) it is possible to obtain the coordinates of the object in the *heliocentric ecliptic system*.

$$L = \begin{bmatrix} cos(\Omega) & -sin(\Omega) & 0 \\ sin(\Omega) & cos(\Omega) & 0 \\ 0 & 0 & 1 \end{bmatrix} \begin{bmatrix} 1 & 0 & 0 \\ 0 & cos(i) & -sin(i) \\ 0 & sin(i) & cos(i) \end{bmatrix} \begin{bmatrix} cos(\omega) & -sin(\omega) & 0 \\ sin(\omega) & cos(\omega) & 0 \\ 0 & 0 & 1 \end{bmatrix} \tag{5.6}$$

$$r = \begin{Bmatrix} x \\ y \\ z \end{Bmatrix} = [L] \begin{Bmatrix} x_p \\ y_q \\ 0 \end{Bmatrix} \tag{5.7}$$

5.2 Comparison

In order to evaluate how much the real trajectory differs from the unperturbed trajectory, obtained thanks to the normal propagation for hyperbolic trajectory, as described above, it is necessary to take the state vectors from the JPL site [**1**]. In Figure *5.1* it is possible to see the two trajectories compared.

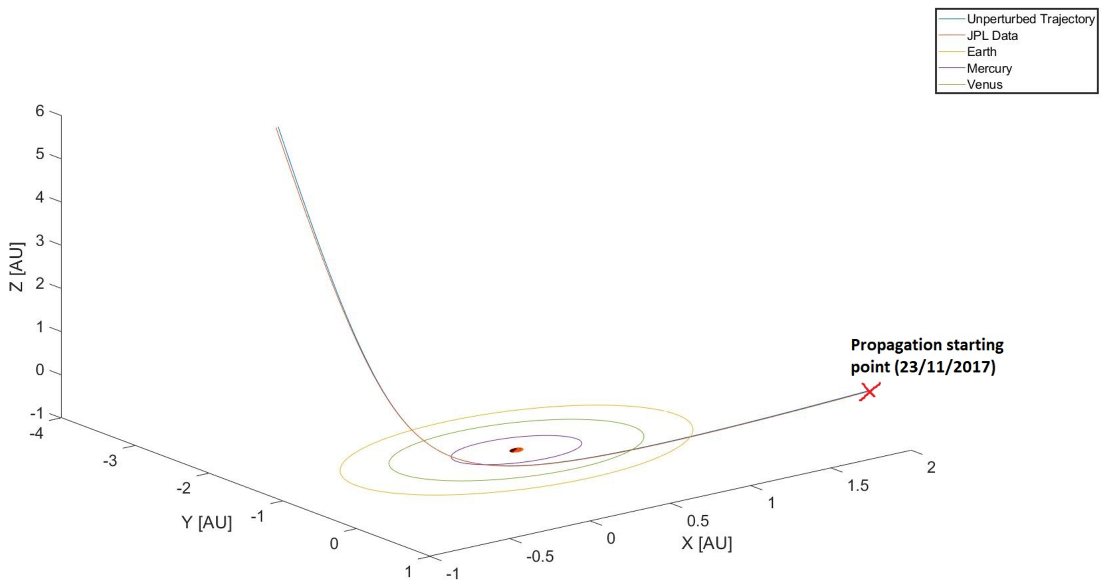

Figure 5.1: Comparison between JPL data and unperturbed trajectory.

It is possible to notice that the two trajectories do not differ much, this means that the extent of the perturbations will not be high; it is also possible to compare the data obtained from the JPL site with the perturbed trajectory in the low density SRP case (with $\rho = 10^{-5} kg/m^3$), as show in Figure *5.2* :

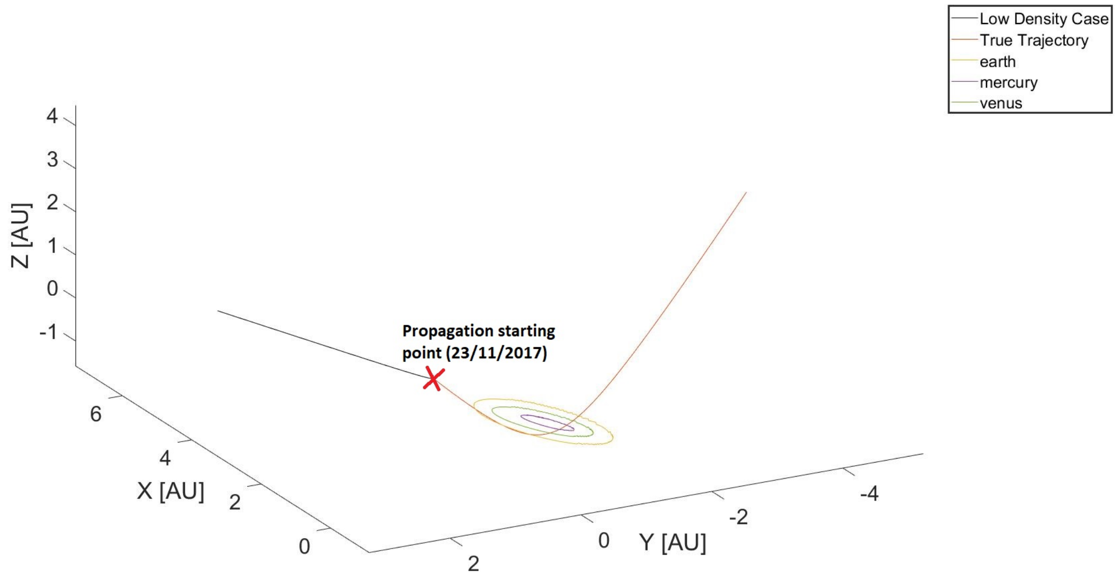

Figure 5.2: Comparison between real data and low density SRP case.

It is possible to see in Figure *5.1* that the two trajectories are very similar, while in Figure *5.2* the two trajectories are completely different. In fact these two start from the same propagation point, but the trajectory perturbed by the effect of solar radiation, after an initial inflection, propagates in a completely different direction.
We can come to the conclusion that the perturbances can not be high; the hypothesis of very low density ($\rho = 10^{-5} kg/m^3$) is not valid anymore, because it leads to very high perturbances due to *solar radiation pressure* with a great difference between real and unperturbed orbit.

Chapter 6

Analysis

In this chapter the code used for the propagation of the orbit of *Asteroid Oumuamua* will be explained. Cowell's method and Runge Kutta integration method are used for the propagation of the trajectory and are considered among the perturbations the solar radiation pressure and the third-body perturbation . From Equation (4.1) it is possible to explicitly write the equation for the total acceleration, as in Equation (6.1):

$$\ddot{\bar{r}} = -\frac{\mu_s}{|\bar{r}^3|} - \mu_p[\frac{\bar{r}_{pa}}{|\bar{r}_{pa}^3|} - \frac{\bar{r}_{ps}}{|\bar{r}_{ps}^3|}] + P\frac{S}{m}(\frac{d_{min}}{|\bar{r}|})^2\frac{\bar{r}}{|\bar{r}|} \tag{6.1}$$

$\bar{r}_{pa}$ is the vector from the perturbative planet to the asteroid, $\bar{r}_{ps}$ is the vector from the perturbative planet to the Sun, P is as in Equation (**??**), calculated at the minimum distance from the Sun.
The propagation was started at 23/11/2017, the epoch of the avaiable Keplerian elements and initial state vector of the object **[1]**. In order to have for every epoch the position of the planets refers to the Sun, an unperturbed propagation has been made for these planets, in order to calculate the perturbative acceleration.
The propagation has been made for the both the disc-shape and cigar-shape in best and worst case of the object's orientation to the Sun, for the calculation of the solar radiation pressure.

6.1 1 Year Propagation

First, a backward propagation over 1 year has been made, in order to evaluate the trajectory during the period of minimum distance to the inner planets and Sun. It is possible to see the results for the different case in Figures *6.1* :

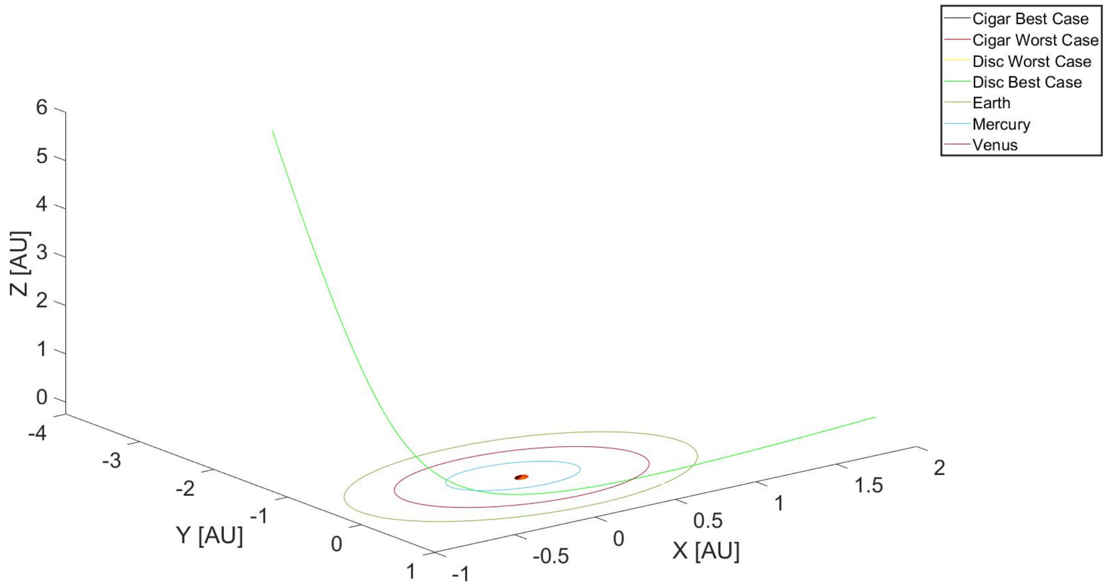

Figure 6.1: Propagation for 1 year, comparison of all cases.

Since the 4 cases are very similar, in Figure *6.1* the trajectories overlap; in Figure *6.2* it is possible to see a detail of the Figure *6.1*, showing the different trajectories:

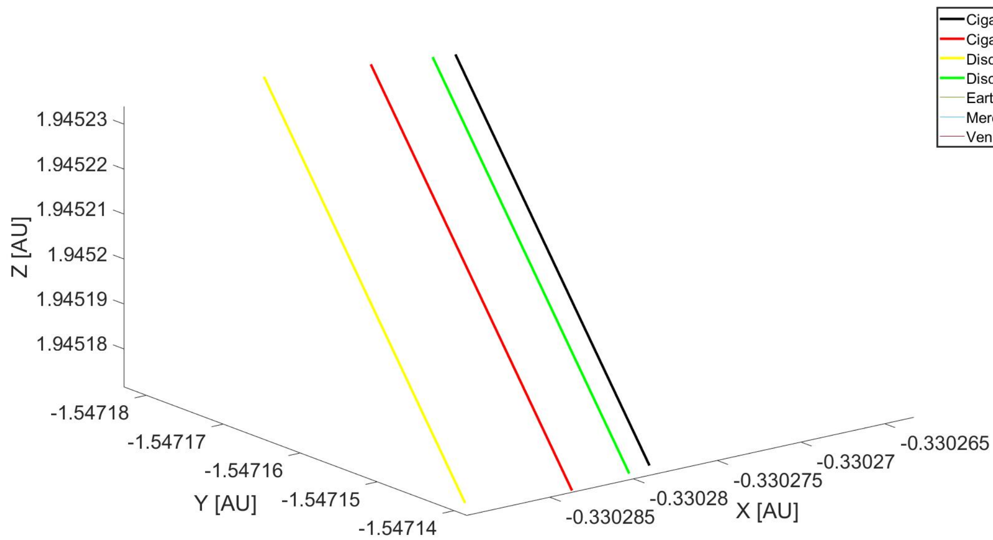

Figure 6.2: Propagation for 1 year, detail of the comparison of all cases.

It is possible to see that the trajectories in the different scenarios do not differ much from each other; in order to have an idea of the error between the different cases, in Figure *6.3* the percentage errors are represented. Every single percentage error has been calculated as the distance's error between two different cases, divided by the avarage distance from the Sun for the two cases. In these cases the error is very low, the maximum is $1 * 10^{-3}\%$, during the passage at the perihelion (i.e. at 75 days befor the epoch of the initial state vector).

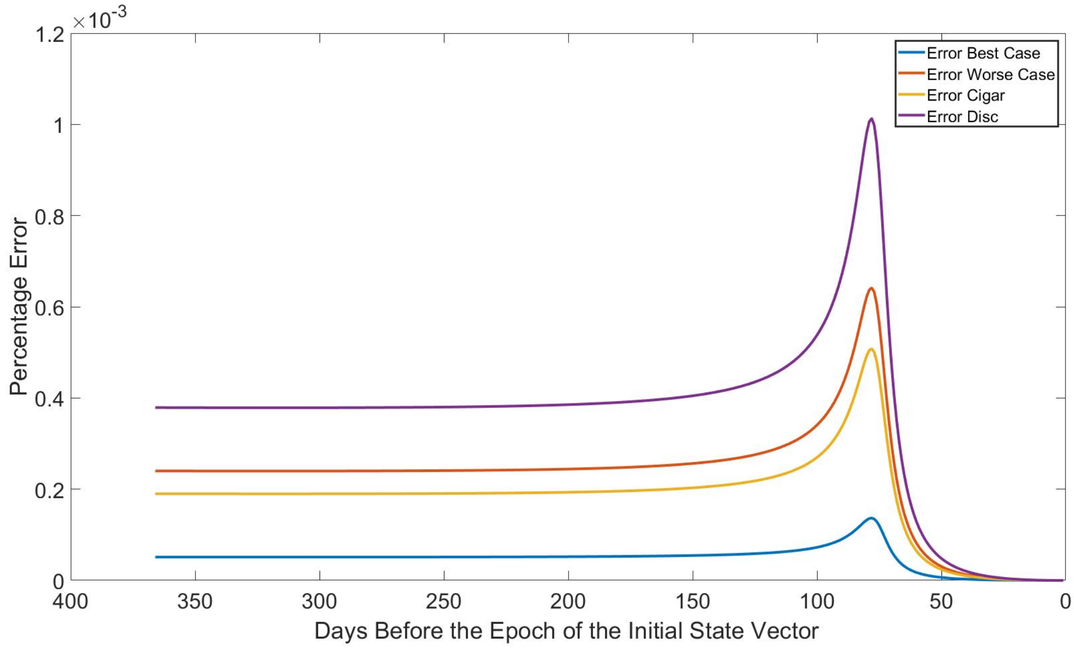

Figure 6.3: Propagation for 1 year, percentage error

6.2 165 Years Propagation

Next, the backward propagation has been made for 165 years, in order to show an entire rotation of all the planets arount the Sun (Neptune has a revolution period of 165 years); the results are shown in Figure *6.4* :

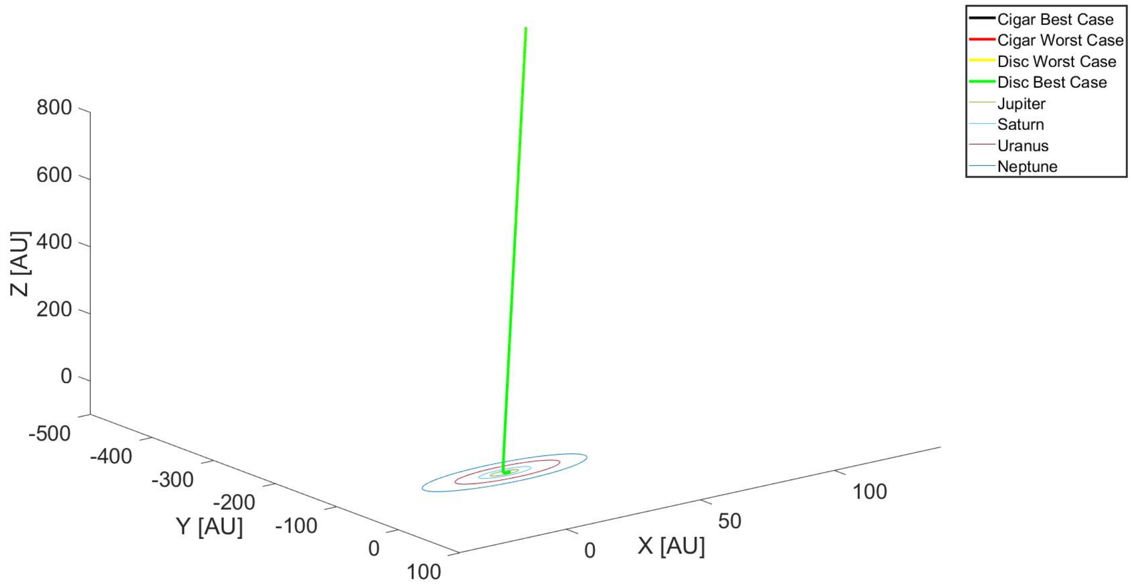

Figure 6.4: Propagation for 165 years, comparison of all cases.

As before, the 4 cases are very similar, in Figure *6.4* the trajectories overlap; in Figure *6.5* it is possible to see a detail of the Figure *6.4*, showing the different trajectories:

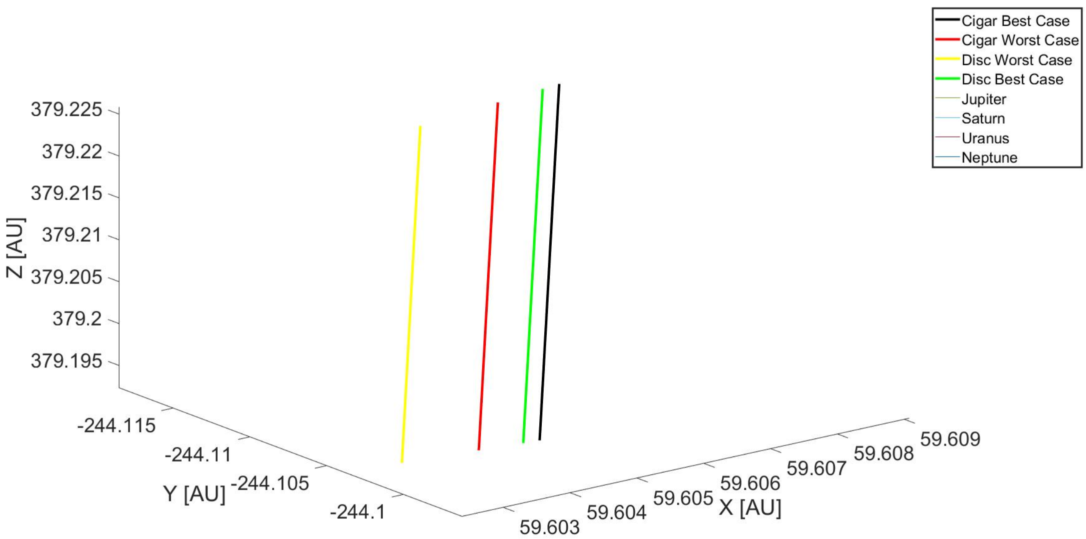

Figure 6.5: Propagation for 165 years, detail of the comparison of all cases.

Even for this propagation the different trajectories are almost entirely coincident; in Figure *6.6* it is possible to see that the maximum percentage error is very close to the starting point (in fact it coincides with the point found in the Figure *6.3* , i.e. at 75 days befor the epoch of the initial state vector) and the percentage error converges to a value just over $0.4 * 10^{-3}\%$ at ”infinity”.

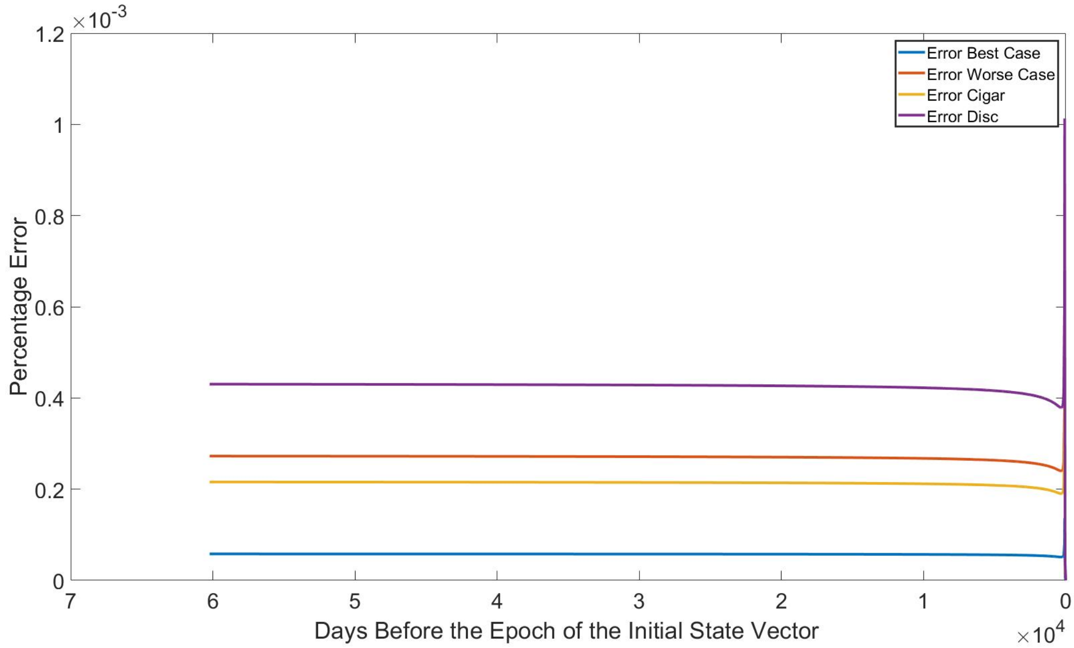

Figure 6.6: Propagation for 165 year, percentage error

Chapter 7

Conjunction Analysis

After obtaining the trajectory of Oumuamua it is possible to use this data for another purpose, in order to evaluate if this object had a conjunction with another object in the Solar System backwards in time. To do this, a group of Solar System objects has been isolated and used as candidates as possible "Origin Home" for Oumuamua. Due to the huge number of objects present in our Solar System, it was necessary to use a method to select a large number of candidates to analyze. Since Oumuamua has a high inclination and a high semi-major axis, objects with characteristics that made possible a conjunction with the asteroid in question were selected; in particular, since in a short time Oumuamua acquires a high value of component z of the state vector, objects belonging to the inner Solar System and objects that have a high inclination have been selected.
In this way 580 objects, mainly asteroids, were selected, which are possible candidates to be an origin for Oumuamua. For anyone of them a backwards propagation was carried out, without considering perturbative effects.

7.1 Kepler Problem

Thanks to **[1]** it is possible to obtain the Mean Anomaly and the orbital paramenters for every candidate at the epoch of the initial state vector used to start the propagation of Oumuamua. In this case we have to solve the inverse problem: we have a known period of time and starting anomaly, and we want to obtain the new anomaly after that period of time.
Using Equation (7.1) it is possible to find the Mean Anomaly for every period of time.

$$M = \sqrt{\frac{\mu}{a^3}}t \tag{7.1}$$

Using Equation (7.2) it is possible to calculate the Eccentric Anomaly by applying it to the Newton method;

$$M = E - e * sin(E) = f(E) \tag{7.2}$$

The Newton method (aalso known as Newton-Raphson method) is a root-finding algorithm, which produces approximations to the roots of a function in a iterative way, where each subsequent root is better. M is the starting value for E(0) and the value E(1) is found by Equation (7.5):

$$E(1) = E(0) - \frac{f(E(0)) - M}{f'(E(0)} \tag{7.3}$$

with

$$f'(E) = 1 - e * cos(E(0)) \tag{7.4}$$

This process has to be repeted using general Equation (7.5) until the difference of two subsequent roots is below a certain tolerance.

$$E_{k+1} = E_k - \frac{f(E_k) - M}{f'(E_k)} \tag{7.5}$$

Once the Eccentric Anomaly is obtained, thanks to Equation (7.6), which is obtained by the geometric relation between circle and ellipse, it is possible to obtain the True Anomaly (ν);

$$\nu = atan(\frac{\sqrt{1-e^2} * sin(E)}{cos(E) - e}) \tag{7.6}$$

With the True Anomaly the component of the range in the Perifocal Plane can be found with Equation (5.5); in this reference system the x-axis points towards the periapsis of the orbit, the y-axis is rotated over 90 degrees and both are in the plane of the orbit; the frame is centered at the celestial body at which the orbit is centered.
Finally, by applying Equations (5.6) and (5.7) it is possible to obtain the three-dimensional position at any epoch for all the candidates.

7.2 Candidates

In order to evaluate the origin of Oumuamua it is necessary to isolate a group of objects present in the Solar System and propagate them backwards in time by carrying out a conjunction analysis between them and Oumuamua in order to calculate their minimum distance. Since Oumuamua exhibits a high increase in the z-component in a short time, objects belonging to the inner Solar System and objects that have a high semi-major axis and / or a high inclination have been selected.
Using this methodology, 580 candidates were isolated and analyzed and it is possible to find the complete list and their MD from Oumuamua in Appendix A.

7.3 Analysis of the Results

Thanks to the propagation of all the 580 candidates it is possible to obtain for every one of them, the minimum distance (MD) from asteroid Oumuamua at some epoch; in Figure *7.1* are represented all the MD for all the candidates. Most of them has a MD under 20 AU but there are cases where this value

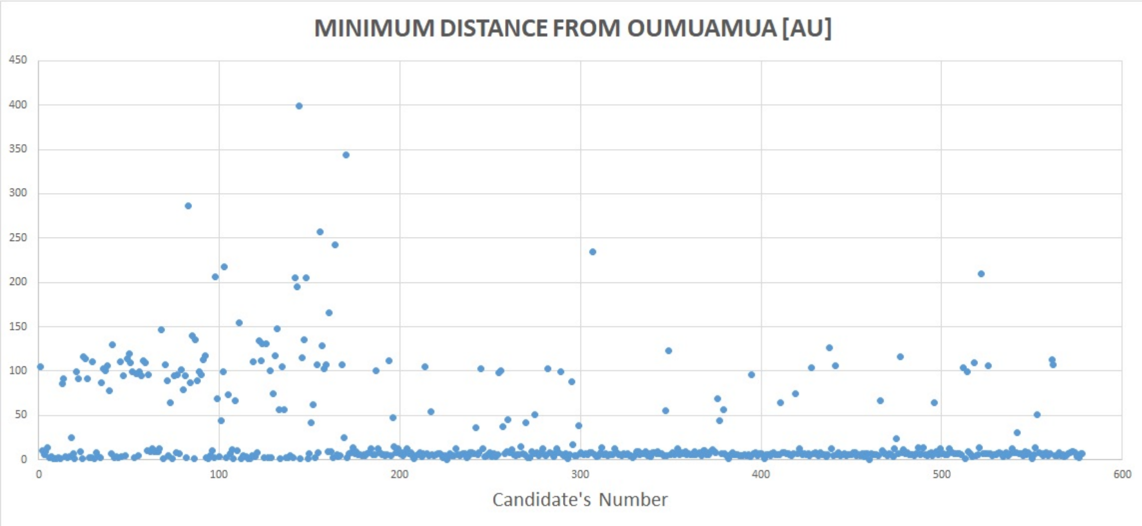

Figure 7.1: Minimum distance w.r.t. Oumuamua for all the candidate origin objects.

is highly above 100 AU. In the Index there are all the candidates with the respective minimum distance.

In order to have a better understanding of which of them could be a possible candidate, the analysis has been divided in two blocks: considering first the candidates which have an MD of less than 1 AU, and then the ones which have an MD between 1 and 2 AU.

7.3.1 Closest Candidates

Among all the candidates, only 4 have a minimum distance under 1 AU and they are listed in Table *7.1*:

Candidate	MD [AU]	Epoch of MD	MD uncertainty [AU]
1994WR12	0.987	21/09/2017	$9.3*10^{-7}$
1998RO1	0.968	24/09/2017	$7.6*10^{-7}$
Atira	0.4492	08/09/2017	$2.5*10^{-6}$
Moshup	0.4286	04/09/2017	$3*10^{-6}$

Table 7.1: Closest candidates and characteristics of closest approach

In this table are shown the MD, the epoch of the minimum approach and the error obtained by considering different configurations for the asteroid at that specific epoch. As we can see, the minimum approach is very early in the propagation; this is obvious because all these candidates are inner Solar System objects and their MD happened when asteroid Oumuamua was very close to the Sun. Even if their MD happened not long before the epoch of the initial state vector, the first discovery of this asteroid was the 18th of October 2017 and we do not know what happened to the asteroid before that date.
If we compare the MD with the uncertainty of the propagation, none of these

objects seem to be a plausible origin for asteroid Oumuamua. For further confirmation, an analysis on the state vector of the single candidates has been done; considering the period of revolution of the candidates and their epoch of minimum approach to the asteroid, it is possible to compare the components of the state vector before and after the MD using a time span equal to the period of revolution. If there was an event that led to the separation of the asteroid from the main body, one can expect variations in the characteristics of the primary body and therefore on its state vector. All of these data were taken from **[1]**. In Figure *7.2* are shown the characteristics of the candidates and the errors of the state vectors:

CANDIDATE	STATE VECTOR BEFORE MATCH [km,km/s]			STATE VECTOR AFTER MATCH [km,km/s]			EPOCH OF MINIMUM APPROACH	PERIOD [days]	TIME SPAN	ADIMENSIONAL ERROR
1994wr12	X 3.31E+07	Y -6.18E+07	Z -6.95E+06	X 3.11E+07	Y -6.22E+07	Z -6.78E+06	21/09/2017	241	26/01/2017	2.98E-02
	VX 4.76E+01	VY 1.72E+01	VZ -4.14E+00	VX 4.81E+01	VY 1.62E+01	VZ -4.24E+00			24/09/2017	2.08E-02
1998ro1	X -4.63E+07	Y -3.40E+07	Z -1.71E+07	X -4.67E+07	Y -3.22E+07	Z -1.65E+07	24/09/2017	361	01/10/2016	3.17E-02
	VX 8.89E+00	VY -5.41E+01	VZ -2.19E+01	VX 8.14E+00	VY -5.46E+01	VZ -2.21E+01			27/09/2017	1.62E-02
Atira	X -6.36E+07	Y 1.04E+08	Z 1.79E+07	X -6.37E+07	Y 1.04E+08	Z 1.79E+07	08/09/2017	233	21/01/2017	2.05E-03
	VX -2.69E+01	VY -7.70E+00	VZ 1.34E+01	VX -2.69E+01	VY -7.69E+00	VZ 1.34E+01			11/09/2017	6.15E-04
Moshup	X -5.80E+05	Y 2.95E+07	Z -1.07E+07	X -6.74E+06	Y 2.85E+07	Z -1.47E+07	04/09/2017	189	02/03/2017	2.37E-01
	VX -6.97E+01	VY -7.06E+00	VZ -4.85E+01	VX -6.82E+01	VY -1.77E+01	VZ -4.37E+01			07/09/2017	1.38E-01

Figure 7.2: State Vector Analysis

The adimensional error has been calculated by dividing the error obtained for the different components by the medium value of the state vector's component. In Figure *7.3* are shown the MD and adimensional error for these candidates:

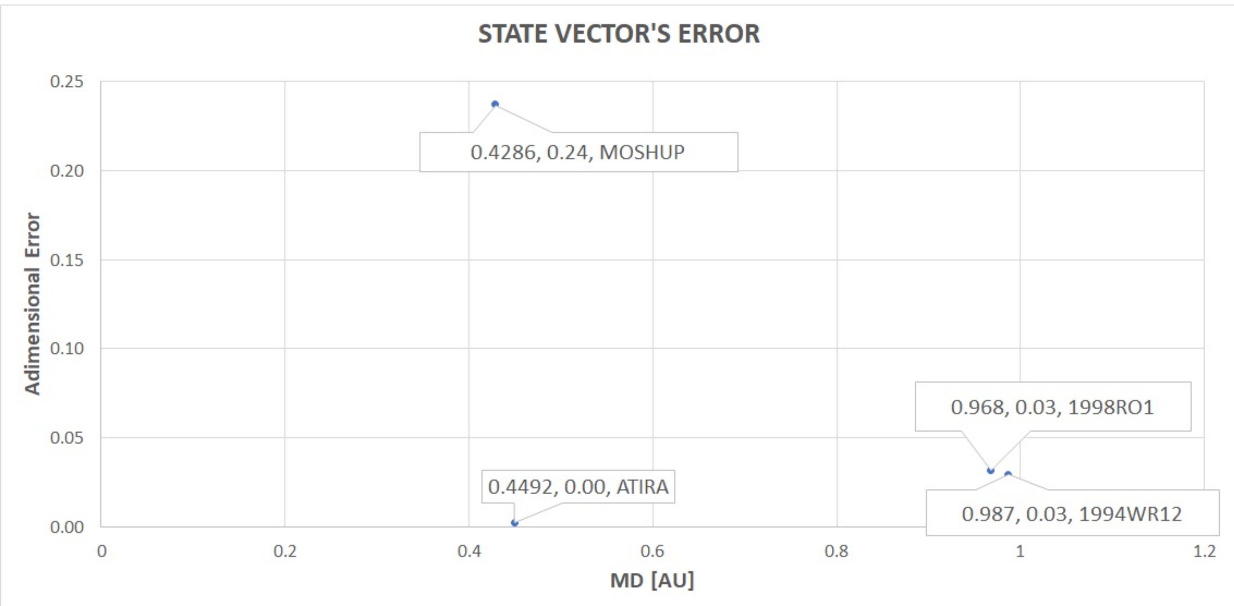

Figure 7.3: Error-MD plot of closest possible conjunctions.

As we can see none of these have big uncertainties in the state vectors and

they are not close enough to the asteroid to be considered as the origin of Oumuamua.
In Figures *7.4*, *7.5*, *7.6* and *7.7* the trajectory of the 4 candidates are represented.

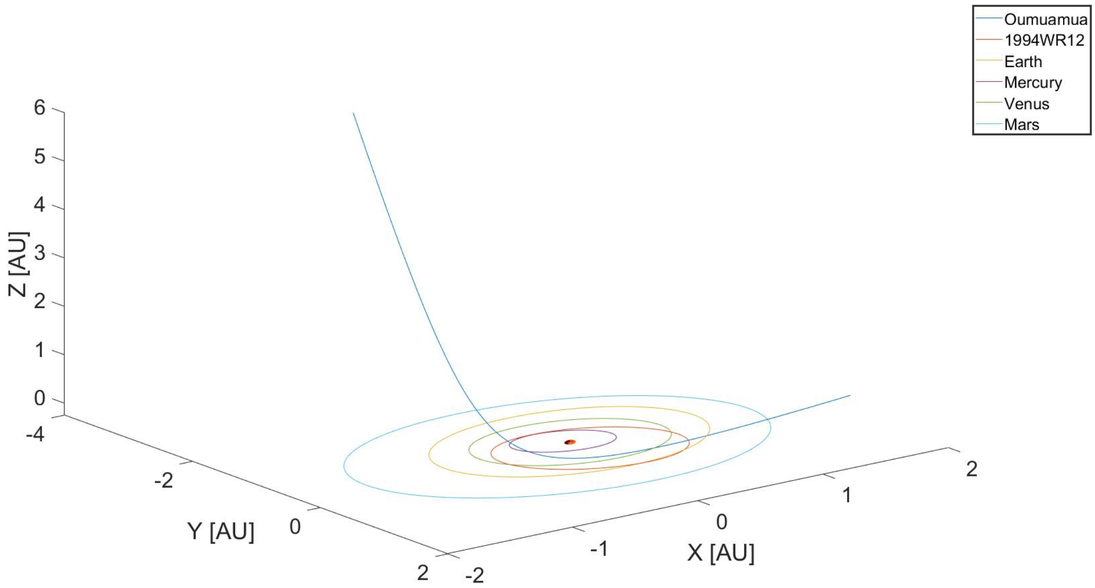

Figure 7.4: 1994WR12 trajectory.

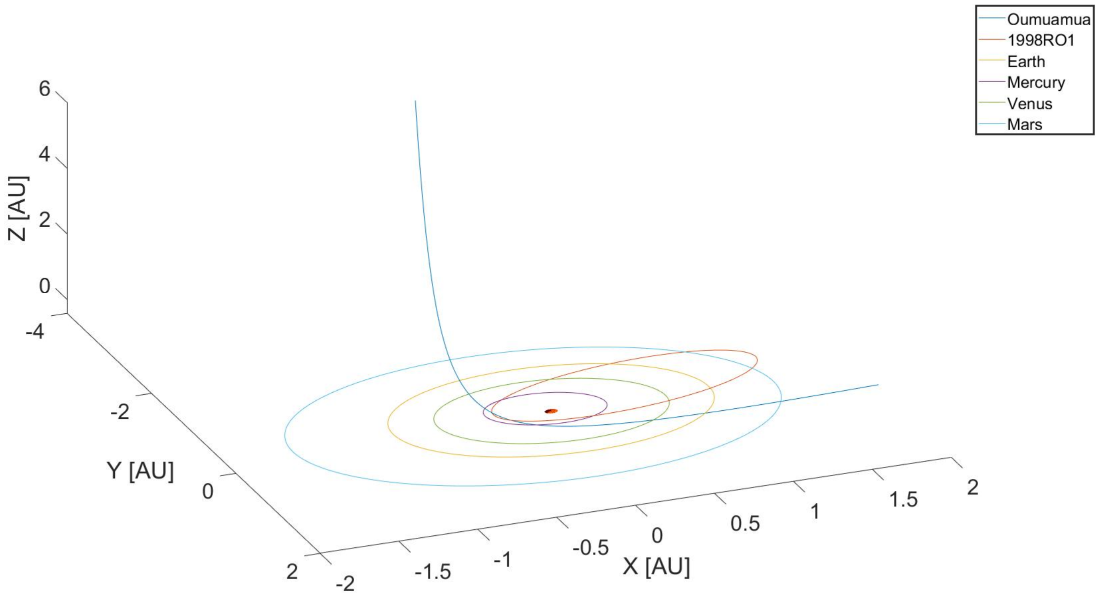

Figure 7.5: 1998RO1 trajectory.

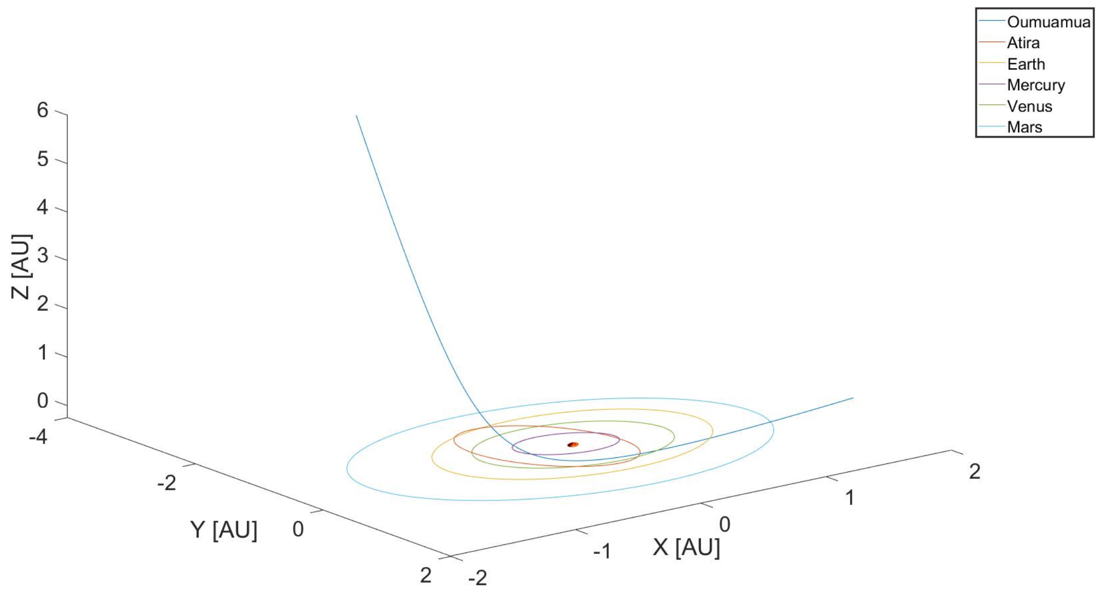

Figure 7.6: Atira trajectory.

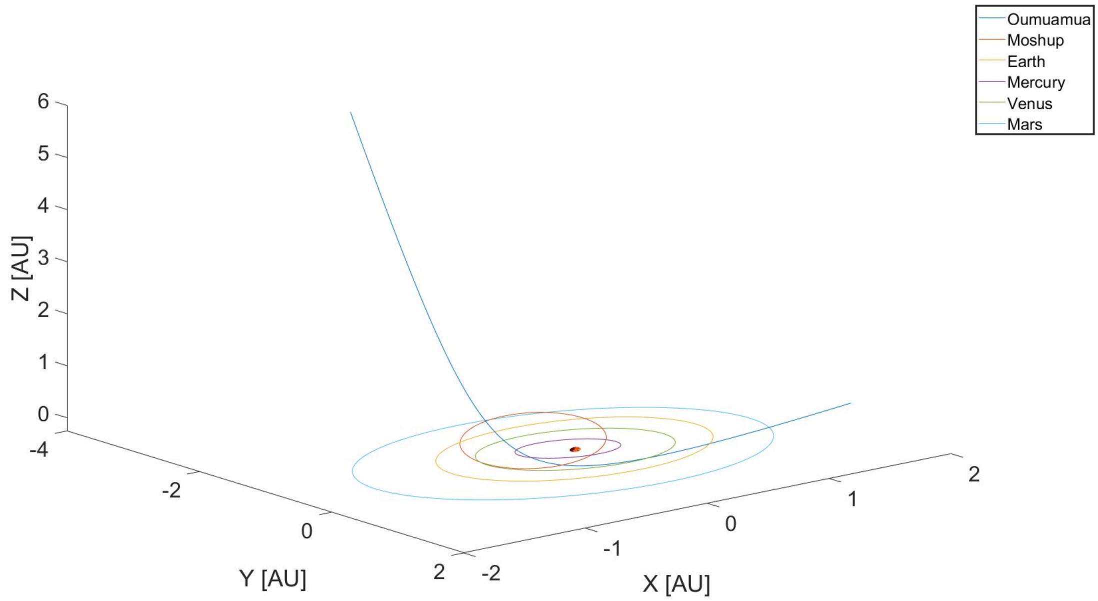

Figure 7.7: Moshup trajectory.

It is possible to see that all the four candidates are inner Solar System objects, since their trajectories are almost entirely included within the orbit of Mars.

7.3.2 Other Candidates

After studying the closest candidates, none of them were found that could be responsible for the origin of the asteroid; therefore, the analysis was carried out on candidates whose MD is between 1 and 2 AU. In this case there are 22 possible candidates which are shown in Table *7.2*; also in this table there is the MD, epoch of MD and the uncertainty calculated on the different cases of study. In this case if the MD is compared to the error (for every single candidate) it is possible to notice that these two values have very different orders of magnitude.

Candidate	MD [AU]	Epoch of MD	MD uncertainty [AU]
1989JA	1.9585	11/10/2017	$2.7*10^{-7}$
1989JA	1.8736	14/08/2017	$4.5*10^{-6}$
1992FE	1.9288	29/09/2017	$5.6*10^{-7}$
1998WT24	1.9795	28/08/2017	$3.5*10^{-6}$
2000SG344	1.9651	17/10/2017	$1.8*10^{-7}$
2003SD220	1.4921	30/09/2017	$5.3*10^{-7}$
2004FH	1.384	29/09/2017	$5.6*10^{-7}$
2005GO21	1.9783	03/10/2017	$4.4*10^{-7}$
2005YU55	1.9632	17/10/2017	$1.8*10^{-7}$
2008EV5	1.9948	15/10/2017	$2.1*10^{-7}$
2008TC3	1.5963	06/09/2017	$2.8*10^{-6}$
2009TM8	1.9755	01/09/2017	$3.2*10^{-6}$
2010AL30	1.6291	30/09/2017	$5.3*10^{-7}$
2011CQ1	1.7484	29/08/2017	$3.4*10^{-6}$
2013YP139	1.9031	25/08/2017	$3.7*10^{-6}$
2014HQ124	1.978	17/09/2017	$1.2*10^{-6}$
APOPHIS	1.9588	16/10/2017	$2*10^{-7}$
DUENDE	1.8771	14/10/2017	$2.2*10^{-7}$
ICARUS	1.9703	05/08/2017	$5.2*10^{-6}$
KAMOOALEWA	1.9823	07/09/2017	$2.6*10^{-6}$
RA SHALOM	1.4949	01/110/2017	$5*10^{-7}$
TORO	1.9879	15/08/2017	$4.4*10^{-6}$

Table 7.2: 1-2 AU candidates and MD characteristics

Also for these candidates the MA happened not long before the state vector's epoch, that is because all these candidates are inner Solar System objects; as before, a study on the state vector of all the candidates has been done, comparing the state vector before and after the epoch of MA, with a time span equal to the period of revolution of any single object. The results of this analysis are shown in Figure *7.8*.

CANDIDATE	STATE VECTOR BEFORE MATCH						STATE VECTOR AFTER MATCH						EPOCH OF MINIMUM APPROACH	PERIOD [days]	TIME SPAN	ADIMENSIONAL ERROR
1989ja	X	4.02E+07	Y	-1.28E+08	Z	-2.62E+07	X	4.18E+07	Y	-1.27E+08	Z	-2.65E+07	11/10/2017	861	06/06/2015	1.62E-02
	VX	3.49E+01	VY	1.34E+01	VZ	-6.57E+00	VX	3.48E+01	VY	1.37E+01	VZ	-6.50E+00			14/10/2017	9.31E-03
1989va	X	9.24E+07	Y	-1.11E+07	Z	4.06E+07	X	9.21E+07	Y	-1.11E+07	Z	4.06E+07	14/08/2017	228	01/01/2017	3.04E-03
	VX	2.73E+01	VY	2.57E+01	VZ	8.55E-01	VX	2.74E+01	VY	2.57E+01	VZ	8.88E-01			17/08/2017	2.12E-03
1992fe	X	6.93E+07	Y	-9.03E+07	Z	-8.45E+05	X	6.92E+07	Y	-8.99E+07	Z	-8.02E+05	29/09/2017	327	09/11/2016	3.77E-03
	VX	1.91E+01	VY	3.16E+01	VZ	2.93E+00	VX	1.91E+01	VY	3.17E+01	VZ	2.92E+00			02/10/2017	1.00E-03
1998wt24	X	-1.18E+07	Y	1.42E+08	Z	4.12E+06	X	-1.28E+07	Y	1.42E+08	Z	4.23E+06	28/08/2017	223	22/03/2017	6.57E-03
	VX	-2.32E+01	VY	-9.15E+00	VZ	2.80E+00	VX	-2.32E+01	VY	-9.36E+00	VZ	2.80E+00			31/10/2017	8.60E-03
2000sg344	X	-4.12E+07	Y	-1.48E+08	Z	2.43E+05	X	-4.14E+07	Y	-1.48E+08	Z	2.47E+05	17/10/2017	353	01/11/2016	2.42E-03
	VX	2.71E+01	VY	-8.76E+00	VZ	2.78E-02	VX	2.71E+01	VY	-8.76E+00	VZ	2.79E-02			20/10/2017	1.51E-04
2003sd220	X	-4.56E+07	Y	-8.52E+07	Z	-7.77E+06	X	-4.57E+07	Y	-8.50E+07	Z	-7.75E+06	30/09/2017	275	01/01/2017	2.38E-03
	VX	3.52E+01	VY	-1.95E+01	VZ	5.02E+00	VX	3.52E+01	VY	-1.95E+01	VZ	5.02E+00			03/10/2017	6.72E-04
2004fh	X	3.11E+07	Y	-8.55E+07	Z	-2.43E+04	X	3.34E+07	Y	-8.39E+07	Z	-1.96E+04	29/09/2017	271	04/01/2017	3.04E-02
	VX	3.77E+01	VY	1.99E+01	VZ	1.56E-02	VX	3.74E+01	VY	2.09E+01	VZ	1.57E-02			02/10/2017	2.42E-02
2005go21	X	4.30E+07	Y	-1.25E+08	Z	1.69E+07	X	4.32E+07	Y	-1.25E+08	Z	1.72E+07	03/10/2017	239	09/02/2017	5.01E-03
	VX	2.05E+01	VY	1.69E+01	VZ	9.87E+00	VX	2.04E+01	VY	1.70E+01	VZ	9.85E+00			06/10/2017	5.42E-03
2005yu55	X	-7.79E+07	Y	-1.02E+08	Z	-2.42E+05	X	-7.69E+07	Y	-1.01E+08	Z	-2.42E+05	17/10/2017	455	22/07/2016	7.41E-03
	VX	3.45E+01	VY	-1.03E+01	VZ	-1.70E-01	VX	3.47E+01	VY	-1.01E+01	VZ	-1.69E-01			20/10/2017	7.05E-03
2008ev5	X	-1.13E+08	Y	-9.05E+07	Z	1.55E+07	X	-1.13E+08	Y	-9.08E+07	Z	1.54E+07	15/10/2017	343	09/11/2016	3.76E-03
	VX	2.02E+01	VY	-2.18E+01	VZ	-2.46E+00	VX	2.03E+01	VY	-2.16E+01	VZ	-2.48E+00			18/10/2017	6.14E-03
2008tc3	X	1.37E+08	Y	5.34E+07	Z	-4.58E+05	X	1.37E+08	Y	5.35E+07	Z	-4.52E+05	06/09/2017	547	11/03/2016	1.06E-03
	VX	-1.41E+01	VY	2.15E+01	VZ	-1.88E-01	VX	-1.40E+01	VY	2.15E+01	VZ	-1.88E-01			09/09/2017	4.07E-03
2009TM8	X	6.40E+07	Y	1.23E+08	Z	-3.65E+06	X	6.22E+07	Y	1.24E+08	Z	-3.70E+06	01/09/2017	706	29/09/2015	1.64E-02
	VX	-3.29E+01	VY	1.63E+01	VZ	-1.25E+00	VX	-3.31E+01	VY	1.60E+01	VZ	-1.25E+00			04/09/2017	9.09E-03
2010AL30	X	-5.49E+07	Y	-9.66E+07	Z	5.88E+06	X	-5.46E+07	Y	-9.65E+07	Z	5.86E+06	30/09/2017	391	07/09/2016	2.32E-03
	VX	3.12E+01	VY	-2.34E+01	VZ	-1.34E+00	VX	3.13E+01	VY	-2.32E+01	VZ	-1.35E+00			03/10/2017	3.81E-03
2011CQ1	X	1.12E+08	Y	4.32E+07	Z	9.97E+06	X	1.12E+08	Y	4.50E+07	Z	1.01E+07	29/08/2017	280	25/11/2016	1.59E-02
	VX	-5.57E+00	VY	3.34E+01	VZ	1.82E+00	VX	-5.98E+00	VY	3.33E+01	VZ	1.78E+00			01/09/2017	1.31E-02
2013YP139	X	6.87E+07	Y	1.07E+08	Z	1.48E+06	X	6.71E+07	Y	1.09E+08	Z	1.44E+06	25/08/2017	1358	09/12/2013	2.02E-02
	VX	-2.70E+01	VY	3.13E+01	VZ	-1.84E-01	VX	-2.73E+01	VY	3.11E+01	VZ	-1.93E-01			28/08/2017	9.15E-03
2014HQ124	X	7.29E+07	Y	-8.08E+07	Z	4.37E+07	X	7.33E+07	Y	-7.96E+07	Z	4.39E+07	17/09/2017	287	07/12/2016	1.04E-02
	VX	1.69E+01	VY	3.02E+01	VZ	4.95E+00	VX	1.67E+01	VY	3.04E+01	VZ	4.84E+00			20/09/2017	8.25E-03
apophis	X	-1.18E+08	Y	-8.31E+07	Z	1.62E+06	X	-1.17E+08	Y	-8.34E+07	Z	1.67E+06	16/10/2017	324	29/11/2016	3.19E-03
	VX	2.12E+01	VY	-2.05E+01	VZ	1.59E+00	VX	2.13E+01	VY	-2.04E+01	VZ	1.59E+00			19/10/2017	5.58E-03
duende	X	-3.90E+06	Y	-1.29E+08	Z	2.29E+07	X	-3.94E+06	Y	-1.29E+08	Z	2.26E+07	14/10/2017	318	03/12/2016	3.51E-03
	VX	3.19E+01	VY	1.01E+00	VZ	-3.75E+00	VX	3.19E+01	VY	1.51E+00	VZ	-3.84E+00			17/10/2017	1.58E-02
icarus	X	-4.06E+07	Y	-2.57E+07	Z	1.69E+07	X	-4.09E+07	Y	-2.61E+07	Z	1.70E+07	05/08/2017	409	25/06/2016	1.03E-02
	VX	-1.04E+01	VY	-6.48E+01	VZ	3.43E+00	VX	-9.90E+00	VY	-6.45E+01	VZ	3.22E+00			08/08/2017	9.51E-03
kamooalewa	X	1.31E+08	Y	-3.34E+07	Z	-1.82E+07	X	1.31E+08	Y	-3.26E+07	Z	-1.81E+07	07/09/2017	366	09/09/2016	6.42E-03
	VX	6.90E+00	VY	3.20E+01	VZ	8.75E-01	VX	6.80E+00	VY	3.20E+01	VZ	8.96E-01			10/09/2017	3.11E-03
ra shalom	X	-5.65E+07	Y	4.39E+07	Z	-9.51E+06	X	-5.62E+07	Y	4.49E+07	Z	-9.73E+06	01/10/2017	278	30/12/2016	1.46E-02
	VX	-2.57E+01	VY	-4.22E+01	VZ	1.29E+01	VX	-2.61E+01	VY	-4.19E+01	VZ	1.29E+01			04/10/2017	8.69E-03
Toro	X	-2.19E+07	Y	1.33E+08	Z	-2.08E+06	X	-2.18E+07	Y	1.34E+08	Z	-2.04E+06	15/08/2017	585	11/01/2016	3.83E-03
	VX	-3.56E+01	VY	4.55E+00	VZ	-5.81E+00	VX	-3.56E+01	VY	4.61E+00	VZ	-5.81E+00			18/08/2017	1.97E-03

Figure 7.8: State Vector Analysis, 1-2 AU Candidates

The adimensional error has been calculated by dividing the error obtained for the different components by the medium value of the stae vector's component.
In Figure *7.9* the MD and adimensional error for these candidates are shown.

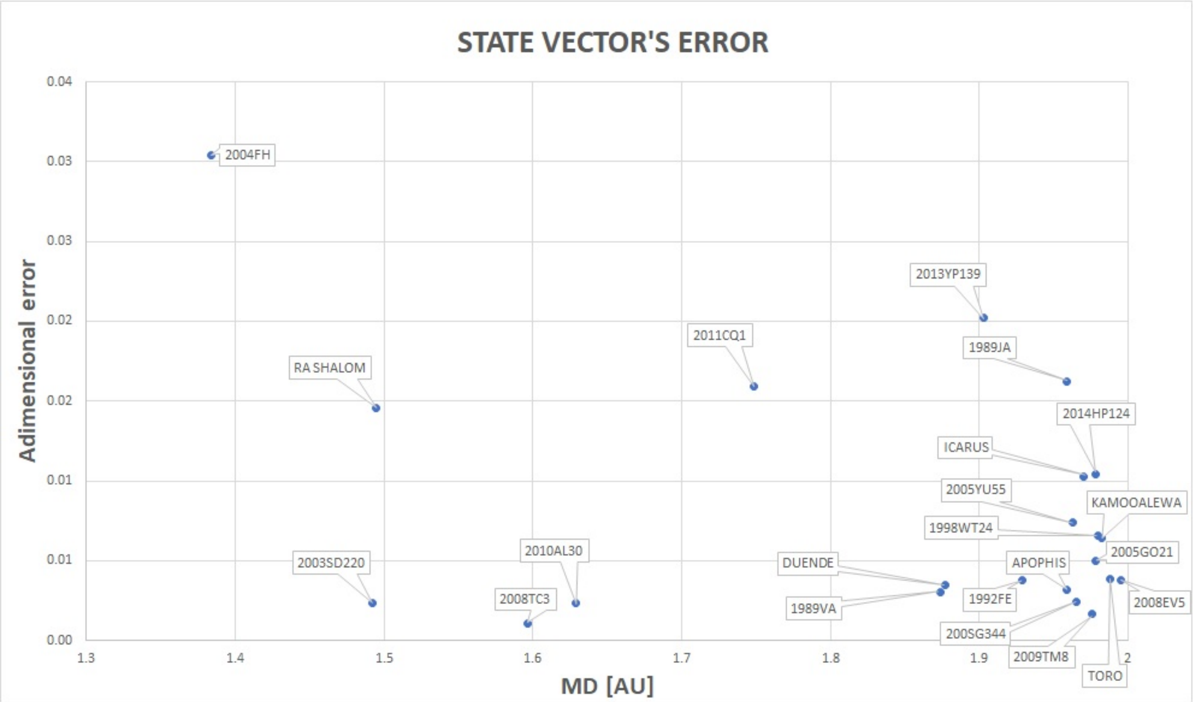

Figure 7.9: Error-MD plot,1-2 AU candidates.

Also in this case, none of the candidates had big uncertainties in the state vectors, making up to the MD values itself, and they were not close enough to the asteroid to be considered the origin of Oumuamua.

7.3.3 High Inclination Candidates

As we can see from the trajectory of Oumuamua, this object has a rapid increase of its z-component and this means that in a short period of time, the asteroid will be far from the ecliptic plane; for this reason a specific analysis has been done on those objects that have a high inclination and high semi-major axis. [**1**] can be used as a source of information on all the objects in the Solar System with an inclination greater than 60° and semi-major axis greater than 15 AU. These candidates are listed in Figure *7.10* and in Figure *7.11*:

CANDIDATES	MINIMUM DISTANCE FROM OUMUAMUA [AU]	EPOCH OF MINIMUM DISTANCE
2002XU93	154.5164	28/08/2005
2007BP102	44.7639	23/11/2017
2008KV42	66.4874	23/11/2017
2010WG9	56.1879	30/06/2016
2011KT19	56.576	23/11/2017
2014LM28	42.2612	23/11/2017

Figure 7.10: High inclination candidates.

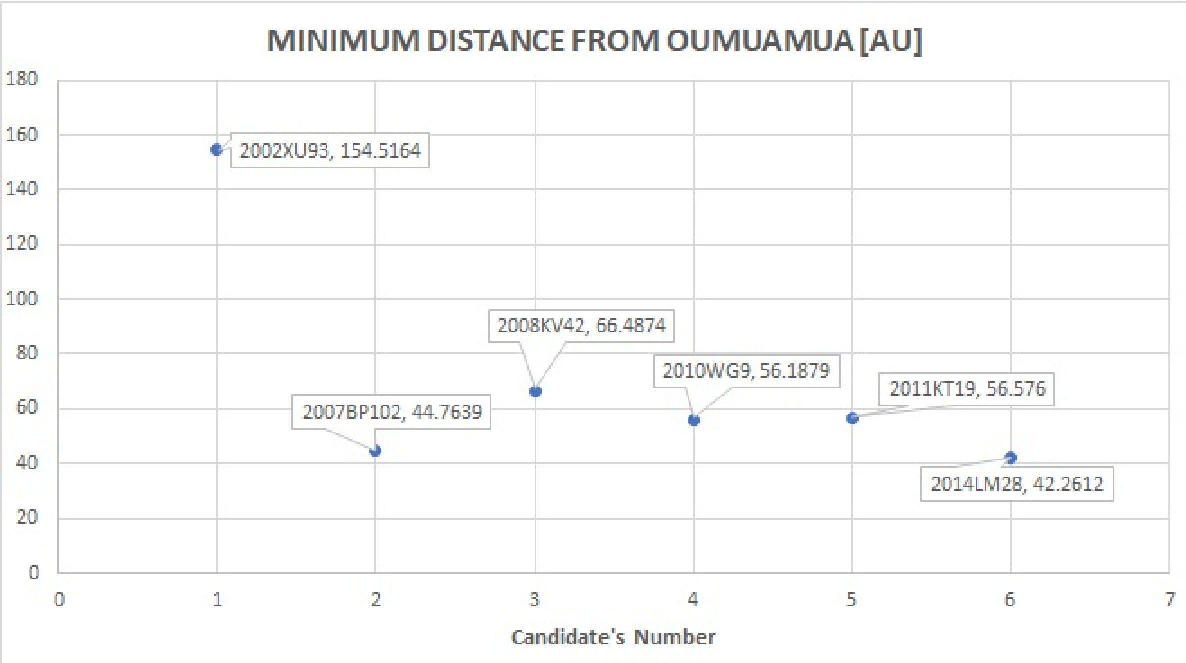

Figure 7.11: High inclination candidates.

All of them have a very high MD from Oumuamua and most of them have the MA at the state vector's epoch (23/11/2017). Therefore, none of these candidates can be a possible origin for the asteroid Oumuamua.

Chapter 8

Conclusions

The purpose of the thesis is to obtain a better understanding of the asteroid Oumuamua; the initial problem was not being aware of the dimensions and characteristics of the object studied, but thanks to the study carried out on the evolution of the light reflected by the body ([**5**]) and thanks to considerations made on its density, it was possible to obtain four different cases of studies that differ in shape (disc and cigar) and orientation of the body with respect to the Sun (obtaining the worst case when the body has its maximum surface facing the Sun and the best case when the minimum surface is facing the Sun).
The next problem was the evaluation of all the perturbations that occur on the object during its passage in the inner Solar System, such as Third Body Perturbation, Solar Radiation Pressure, Atmospheric Drag; for this reason, several calculations were made in order to quantify these perturbations and to be able to evaluate their effect by comparing them with the gravitational acceleration provided by the Sun.
After evaluating these effects, the next step was to chose a perturbation techniques and an integration method to apply to Oumuamua in order to have a complete trajectory; thanks to that, a preliminary analysis was carried out on the asteroid, comparing the data available on the JPL site with a normal propagation for the hyperbolic trajectory and obtaining results that show that the low-density case is not a feasible scenario.
Finally, a conjunction study was made on Oumuamua and all the candidate objects in order to evaluate if any of the candidates is a possible origin for the analyzed asteroid; the analyses show that even if some of the candidates have a relatively low MD, the comparison with the uncertainty obtained by the studies of different cases and the studies carried out on the state vector of the candidates, none of the studied object is a possible origin for Oumuamua. This conclusion holds to the considered 580 Solar System objects and the 6 high-inclination asteroids.
In order to have a better understanding of the studied asteroid, the future developments of the project can be a further conjunction analysis between Oumuamua and other candidates selected with additional criteria, perhaps considering objects outside the Solar System.

Bibliography

[1] https://ssd.jpl.nasa.gov/sbdb.cgi#top *[25/02/2020]

[2] https://theskylive.com/3dsolarsystem?obj=oumuamua *[25/02/2020]

[3] https://en.wikipedia.org/wiki/Radiation_pressure *[25/02/2020]

[4] https://en.wikipedia.org/wiki/%CA%BBOumuamua *[25/02/2020]

[5] Modeling the light curve of ‘Oumuamua: evidence for torque and disc-like shape, Sergey Mashchenko, 13 September 2019, Monthly Notices of the Royal Astronomical Society, Volume 489, Issue 3, November 2019, Pages 3003-3021

[6] Fundamentals of Astrodynamics, Roger R. Bate Donald D. Mueller Jerry E. White, Dover Publications, INC., New York, 1971

[7] https://en.wikipedia.org/wiki/(528219)_2008_KV42 *[25/02/2020]

[8] https://en.wikipedia.org/wiki/Coma_(cometary) *[25/02/2020]

[9] https://en.wikipedia.org/wiki/Orbital_elements *[25/02/2020]

*Date of last access

Appendix A: overview of all inner Solar System objects evaluated for a possible conjunction with Oumuamua, at their minimum distance

CANDIDATES	MINIMUM DISTANCE FROM OUMUAMUA [AU]	CANDIDATES	MINIMUM DISTANCE FROM OUMUAMUA [AU]	CANDIDATES	MINIMUM DISTANCE FROM OUMUAMUA [AU]	CANDIDATES	MINIMUM DISTANCE FROM OUMUAMUA [AU]
229762	104.942	2013yp139	1.9031	Diotima	6.1732	Lydia	6.3363
514107	10.082	2014an55	115.1261	Donaldjohanson	4.5643	Magellan	3.1585
1950da	5.8064	2014ez51	135.3232	Doris	6.9599	Maja	6.4668
1973na	8.9113	2014fc69	204.9795	Duende	1.8771	Makemake	126.3744
1974fv1	14.3136	2014hq124	1.978	Dynamene	6.3208	Makhaon	13.0343
1986da	2.5763	2014jo25	6.7471	Dziewanna	87.8206	Mandeville	5.0957
1988eg	3.3205	2014lm28	600	Echeclus	17.097	Manwe	106.5298
1989ja	1.9585	2014nw65	62.3045	Echo	4.7593	Marianna	6.4294
1989va	1.8736	2014rc	2.4285	Egeria	5.221	Marion	7.8147
1992fe	1.9288	2014um33	107.1813	Elatus	38.8669	Masursky	4.8503
1994cc	2.1675	2014ux10	8.5639	Elektra	8.2463	Mathilde	5.5993
1994wr12	0.987	2014uz224	257.0105	Eleonora	7.4653	Medea	7.1188
1995sn55	86.4051	2014wk509	128.8414	Elpis	5.7143	Medusa	4.9098
1996tl66	91.3334	2014ya50	102.8442	Emma	7.17	Melete	6.3959
1997ae12	4.2348	2015am281	106.8648	Encke 2P	5.6328	Meliboea	5.9219
1998ky26	2.4036	2015hm10	9.7088	Eos	7.9102	Melpomene	5.6266
1998oh	3.3996	2015rr245	166.1542	Erato	8.4222	Merapi	7.7208
1998qe2	25.5505	2015tb145	9.1399	Eris	234.6483	Messalina	7.7208
1998qw2	7.5022	2015tc25	2.7051	Erminia	6.0784	Metis	5.3502
1998ro1	0.968	2015th367	242.5577	Eros	3.235	Midas	6.1779
1998sm165	99.9778	2015xa378	5.5807	Esclangona	4.3924	Minerva	5.1724
1998sn165	91.5926	2016cw30	3.7092	Eucharis	7.739	Miriam	7.0956
1998uq1	9.2728	2017bq6	4.4945	Euforbo	13.3032	Misterrogers	3.6444
1998wt24	1.9795	2017of69	107.7383	Eugenia	6.4673	Mithra	7.2789
1998ww31	116.3717	2017ye5	24.7326	Eukrate	7.0002	Mnemosyne	6.9053
1999cd158	113.9821	2018vg18	343.4772	Euler	4.7306	Moshup	0.4286
1999de9	91.7989	2019as5	2.4423	Eunike	6.1273	Myrrha	7.3247

CANDIDATES	MINIMUM DISTANCE FROM OUMUAMUA [AU]	CANDIDATES	MINIMUM DISTANCE FROM OUMUAMUA [AU]	CANDIDATES	MINIMUM DISTANCE FROM OUMUAMUA [AU]	CANDIDATES	MINIMUM DISTANCE FROM OUMUAMUA [AU]
1999jd6	3.0751	52europa	7.3653	Eunomia	6.3299	Nausikaa	5.9306
1999jm8	2.9993	Abastumani	8.1759	Euphrosyne	5.8796	Nemausa	5.571
2000yw134	110.2948	Achilles	13.72	Eurybates	12.8959	Nemesis	6.2784
2000sg344	1.9651	Adelheid	6.8588	Eurydike	7.7054	Nereus	4.7333
2000eu110	8.6473	Adelinda	9.2277	Eurynome	5.5341	Nessus	66.3151
2000wo107	3.669	Adeona	5.6251	Euterpe	6.0837	Nestor	10.9137
2001au43	2.9425	Adorea	5.6283	Eva	4.4505	Ninina	7.2959
2001fp185	87.1251	Adria	5.3441	Felicitas	7.0133	Niobe	7.3792
2011fw62	103.1374	Aegina	5.622	Feronia	5.6616	Notburga	4.5201
2001qc298	99.9972	Aegle	5.3038	Fides	6.6794	Nuwa	6.7898
2001qf298	106.2708	Aemilia	7.2398	Flammario	5.2489	Nysa	5.6098
2001qg298	77.942	Aethra	7.7332	Flora	4.329	Nyx	3.7999
2001sn263	6.7951	Agamemnon	12.5088	Florence	2.4564	Odysseus	13.1109
2001ur163	129.675	Aglaja	5.5254	Fortuna	5.1373	Okyrhoe	24.1118
2011uw158	2.5283	Alauda	6.4681	Freda	9.5972	Ophelia	7.0286
2001wn5	3.2368	Albion	100.9109	Freia	9.2982	Orcus	116.1108
2001wr1	2.4673	Alcathous	12.1484	Frigga	6.2192	Ornamenta	7.7491
2002aw197	110.3799	Aletheia	8.378	Galatea	7.4739	Orus	12.0881
2002cu11	3.2933	Alexandra	6.1015	Gallia	7.0326	Ottilia	7.1029
2002kx14	94.5525	Alkeste	6.1748	Ganymed	8.8323	Pales	7.9666
2002mn	5.0589	Alkmene	5.3368	Gaspra	4.8989	Pallas	6.4118
2002ms4	113.8253	Althaea	5.6176	Gaussia	7.5108	Palma	5.5171
2002rp120	119.7368	Altjira	112.1357	Geographos	3.4383	Pandora	6.0902
2002tc302	109.2359	Amalthea	4.4516	Gerda	7.8408	Panopaea	4.8244
2002ux25	99.3248	Amycus	48.132	Gerlinde	8.2283	Papagena	7.5493
2002ve68	2.2436	Anchises	14.6502	Germania	6.5841	Paris	13.722
2002vr128	96.7941	Andromache	8.3947	Golevka	9.4203	Parthenope	6.2001
2002vu94	5.0608	Aneas	12.9455	Gudrun	6.824	Patientia	6.7068
2002wc19	99.497	Angelina	6.5272	Gyptis	6.9254	Patroclus	14.295
2002xu93	154.5164	Ani	8.0641	Hal	4.3197	Peitho	5.9166
2002xv93	94.5142	Annefrank	4.467	Hale Bopp	55.1794	Phaethon	5.0606
2002xw93	111.3829	Antigone	8.2967	Harmonia	5.3212	Philomela	6.6206
2003az84	109.5557	Antilochus	12.7822	Haumea	123.2196	Philosophia	8.6902
2003eh1	11.0044	Antiope	6.5988	Hebe	5.4382	Phocaena	4.3316

CANDIDATES	MINIMUM DISTANCE FROM OUMUAMUA [AU]	CANDIDATES	MINIMUM DISTANCE FROM OUMUAMUA [AU]	CANDIDATES	MINIMUM DISTANCE FROM OUMUAMUA [AU]	CANDIDATES	MINIMUM DISTANCE FROM OUMUAMUA [AU]
2003fy128	96.1156	Apl	8.0683	Hecuba	7.933	Pholus	64.67
2003j10	9.1077	Apollo (1862)	3.2225	Hedwig	5.9777	Piazzia	8.8599
2003j12	12.3419	Apophis	1.9588	Hekate	8.4102	Polana	6.1781
2003j2	9.7352	Aquitania	4.6177	Hektor	12.4888	Polymele	12.5051
2003j23	9.2023	Arethusa	6.4913	Helena	5.3966	Polyxena	7.4388
2003j4	9.2351	Argentina	8.582	Helga	7.9987	Polyxo	6.8162
2003j9	12.2712	Ariadne	3.7486	Helio	6.9353	Pomona	6.3475
2003qx113	147.1359	Armida	7.1983	Henrietta	9.2002	Pompeja	5.9833
2003sd220	1.4921	Arrokoth	104.9962	Hera	5.9468	Poulydamas	13.063
2003uz413	107.2804	Arsionoe	7.1875	Herculina	7.6258	Pretoria	9.2817
2003vs2	89.3476	Artemis	4.5782	Hermentaria	6.4683	Princetonia	7.7019
2004b186	4.6764	Asbolus	54.5805	Hermes	6.4016	Prokne	7.6279
2004ew95	64.3006	Asia	6.4043	Hermione	8.972	Proserpina	6.7596
2004fh	1.384	Aspasia	4.9199	Herschel	6.1826	Protogeneia	7.2402
2004gv9	95.2962	Asterope	5.9668	Hertha	6.7286	Psyche	7.0247
2004lg	8.238	Astraea	7.2318	Hesperia	8.4736	Pulcova	6.31
2004nt33	95.6968	Atalante	7.405	Hestia	5.262	Quaoar	104.2206
2004od4	7.361	Ate	5.9964	Hidalgo	10.0811	Ra Shalom	1.4949
2004pf115	101.7082	Aten	2.6017	Hilda	9.895	Rhadamanthus	99.039
2004tt357	79.4683	Athamantis	5.0637	Hippo	6.0527	Rollandia	9.3034
2004ty364	95.4541	Atira	0.4492	Hispania	5.7088	Romulus	6.5867
2004u1	2.5564	Aurelia	4.9606	Hohensteina	9.0973	Ryugu	3.234
2004ux10	286.3856	Aurora	7.4032	Holmes 17P	11.6593	Salacia	109.5292
2004xa192	86.6681	Ausonia	4.3725	Hopi	9.7652	Sappho	4.8017
2004xr190	139.8542	Austia	5.0643	Huenna	7.8829	Scheila	5.7786
2005go21	1.9783	Automedon	12.2599	Huya	68.898	Schwassmann Wachmann	14.2264
2005qu182	135.9985	Balam	5.5172	Hyakutake	44.5262	Sedna	210.2758
2005rm43	89.5662	Bamberga	5.0537	Hygiea	7.094	Semele	7.3909
2005rn43	99.3267	Beatrix	5.6397	Hylonome	56.2538	Sibylla	7.5759
2005rr43	96.5738	Beethoven	7.3854	Hypatia	7.0322	Siegena	7.3735
2005tb190	112.9688	Bellona	7.5077	Ianthe	4.9254	Sila	106.308
2005uq513	117.5618	Bennu	2.293	Icarus	1.9703	Sirona	6.5816
2005wk4	2.4512	Berbericia	5.2627	Ida	6.0903	Siwa	5.0875

CANDIDATES	MINIMUM DISTANCE FROM OUMUAMUA [AU]	CANDIDATES	MINIMUM DISTANCE FROM OUMUAMUA [AU]	CANDIDATES	MINIMUM DISTANCE FROM OUMUAMUA [AU]	CANDIDATES	MINIMUM DISTANCE FROM OUMUAMUA [AU]
2005yu55	1.9632	Bertha	8.1723	Iduna	7.8054	Sophrosyne	5.4316
2006dp14	4.884	Bertholda	8.0439	Ino	6.2235	Steins	6.1404
2006hy51	10.3787	Betulia	6.8512	Interamnia	6.1256	Stereoskopia	7.6204
2006jy26	2.2549	Bienor	36.5264	Io	6.3473	Sylvia	7.6743
2006qh181	206.6517	Boliviana	5.4519	Iphigenia	4.8193	Tanete	7.4978
2006sq372	68.5677	Bononia	7.6456	Irene	4.6785	Tantalus	3.5994
2006su49	3.343	Borasisi	102.856	Iris	4.4184	Tauris	7.2651
2007bp102	44.7639	Borrelly	12.4482	Irmintraud	5.4756	Tempel 9p 1	7.9937
2007jj43	98.9622	Braille	3.645	Isis	5.0267	Tercidina	5.2784
2007or10	217.4949	Brixia	5.1904	Isolda	6.1484	Terpsichore	7.0128
2007pa8	2.1577	Brunhild	6.4737	Itokawa	3.4967	Teucer	12.6441
2007rw10	73.0715	Camilla	8.7437	Ixion	96.149	Thalia	7.8839
2007tu24	6.6166	Camillo	3.4014	Johanna	6.7841	Themis	7.8988
2007vr6	11.6154	Carlova	6.6803	Juewa	7.664	Thereus	31.0641
2008ev5	1.9948	Castalia	3.2135	Julia	4.9716	Thetis	6.5305
2008kv42	66.4874	Ceres	6.3088	Juno	6.789	Thia	7.3346
2008sb85	10.7531	Ceto	98.6132	Kalliope	6.8848	Thisbe	5.3306
2008st291	155.0167	Chaos	101.0971	Kalypso	6.2053	Thule	9.5109
2008tc3	1.5963	Chariklo	37.7004	Kamooalewa	1.9823	Thyra	5.6143
2008ts26	4.4266	Charybdis	7.0843	Kassandra	6.2087	Tisiphone	8.1184
2009fd	3.7688	Chicago	9.5273	Kleopatra	6.187	Tolosa	5.8838
2009rr	3.976	Chiron	45.2829	Klio	4.3359	Toro	1.9879
2009tm8	1.9755	Chloris	7.9891	Klotho	7.3267	Toutatis	6.4647
2010al30	1.6291	Churyumov Garasimenko 67p	11.7559	Klymene	7.8506	Troilus	13.9712
2010eq169	4.4474	Cincinnati	5.4412	Klytia	6.0409	Typhon	50.6425
2010fx86	110.8442	Circe	5.3162	Kolga	6.4826	Ulla	7.8521
2010ga6	3.1533	Comacina	6.5077	Koronis	6.3457	Undina	7.4385
2010j16	8.6434	Comas Sola	5.5144	Kt19	64.767	Urania	5.3284
2010jo179	134.683	Comas Sola 32p	14.582	Kythera	8.1206	Urda	6.8684
2010kz39	111.483	Concordia	6.7131	Lachesis	7.7567	Ursula	8.0068
2010re64	130.9071	Corduba	6.0154	Lacrimosa	6.7901	Vala	5.1824
2010rf12	2.3799	Crantor	42.2325	Laetitia	6.5909	Vanadis	6.6961
2010rf43	130.9655	Cruithne	3.0737	Lamberta	5.4416	Varda	113.3335

CANDIDATES	MINIMUM DISTANCE FROM OUMUAMUA [AU]	CANDIDATES	MINIMUM DISTANCE FROM OUMUAMUA [AU]	CANDIDATES	MINIMUM DISTANCE FROM OUMUAMUA [AU]	CANDIDATES	MINIMUM DISTANCE FROM OUMUAMUA [AU]
2010so16	2.6359	Cuno	2.3859	Laurentia	5.3766	Varuna	107.0783
2010tj	100.6708	Cybele	9.0709	Leda	7.3578	Velleda	5.2919
2010tk7	2.7414	Cyrene	6.5296	Lempo	74.631	Verenia	4.8348
2010ty53	75.0827	Damocles	50.9868	Leto	7.617	Veritas	7.8365
2010vk201	117.417	Danae	7.9984	Leucus	13.0007	Vesta	4.5711
2010vz98	147.3448	Daphne	4.5131	Leukothea	7.8088	Vibilia	6.2042
2010wg9	56.1879	Davida	8.5526	Liberatrix	6.2751	Victoria	4.1417
2011cq1	1.7484	Deiphobus	12.175	Liguria	6.7514	Virginia	4.5851
2011gm27	105.1153	Dembowska	6.2985	Linear 176P	6.346	Weringia	6.907
2011kt19	56.576	Desiderata	4.6279	Littlewood	6.8681	Wild 2	7.7681
2011md	2.1862	Deucalion	103.2272	Litva	4.5233	Winchester	8.77
2011uw158	2.5283	Diana	7.7044	Logos	103.6865	Wirtanen 46p	9.135
2011xc2	4.9817	Dido	6.7922	Lomia	6.8765	Wratislavia	8.1973
2011yq1	3.6105	Didymos	4.2152	Loreley	8.2218	Xanthippe	4.2555
2012tc4	2.7323	Dike	6.9263	Lucina	6.1468	Yorp	2.568
2012vp113	205.1648	Diomedes	13.0162	Lumen	4.999	Zelinda	6.9111
2013fy27	195.0043	Dione	7.9216	Luscina	8.3582	Zephyr	6.5235
2013fz27	398.8873	Dioretsa	99.749	Lutetia	6.2091		